High-mobility group box 1 (HMGB1) mediates DNA methylation preventing genomic instability

Miss Papitchaya Watcharanurak

จุฬาลงกรณ์มหาวิทยาลัย
CHULALONGKORN UNIVERSITY

A Dissertation Submitted in Partial Fulfillment of the Requirements

for the Degree of Doctor of Philosophy in Biomedical Sciences

Inter-Department of Biomedical Sciences

GRADUATE SCHOOL

Chulalongkorn University

Academic Year 2020

Copyright of Chulalongkorn University

โปรตีน HMGB1 เป็นสื่อกลางของดีเอ็นเอเมทิลเลชันในการป้องกันความไม่เสถียรของจีโนม

น.ส.ปพิชญา วัชรานุรักษ์

จุฬาลงกรณ์มหาวิทยาลัย
CHULALONGKORN UNIVERSITY

วิทยานิพนธ์นี้เป็นส่วนหนึ่งของการศึกษาตามหลักสูตรปริญญาวิทยาศาสตรดุษฎีบัณฑิต
สาขาวิชาชีวเวชศาสตร์ สหสาขาวิชาชีวเวชศาสตร์
บัณฑิตวิทยาลัย จุฬาลงกรณ์มหาวิทยาลัย
ปีการศึกษา 2563
ลิขสิทธิ์ของจุฬาลงกรณ์มหาวิทยาลัย

Thesis Title	High-mobility group box 1 (HMGB1) mediates DNA methylation preventing genomic instability
By	Miss Papitchaya Watcharanurak
Field of Study	Biomedical Sciences
Thesis Advisor	Professor Dr. APIWAT MUTIRANGURA, M.D., Ph.D.

Accepted by the GRADUATE SCHOOL, Chulalongkorn University in Partial Fulfillment of the Requirement for the Doctor of Philosophy

..... Dean of the GRADUATE SCHOOL

(Associate Professor Dr. THUMNOON NHUJAK)

DISSERTATION COMMITTEE

..... Chairman

(Assistant Professor Dr. AMORNPUN SEREEMASPUN, M.D., Ph.D)

..... Thesis Advisor

(Professor Dr. APIWAT MUTIRANGURA, M.D., Ph.D.)

..... Examiner

(Professor Dr. PITHI CHANVORACHOTE)

..... Examiner

(Assistant Professor Dr. Chalisa louicharoen Cheepsunthorn)

..... External Examiner

(Associate Professor Dr. Siwanon Jirawatnotai)

จุฬาลงกรณ์มหาวิทยาลัย
Chulalongkorn University

ปพิชญา วัชรานุรักษ์ : โปรตีน HMGB1 เป็นสื่อกลางของดีเอ็นเอเมทิลเลชันในการป้องกันความไม่เสถียรของจีโนม. (High-mobility group box 1 (HMGB1) mediates DNA methylation preventing genomic instability) อ.ที่ปรึกษาหลัก : ศ. ดร.นพ.อภิวัฒน์ มุทิรางกูร

การลดลงของระดับเมทิลเลชันทั้งจีโนม (Global hypomethylation) ส่งเสริมให้เกิดความไม่เสถียรของจีโนมโดยที่จะทำให้มีการสะสมดีเอ็นเอที่ถูกทำลาย ส่งผลให้มีอัตราของการเกิดมิวเทชันเพิ่มขึ้น การที่จะทำให้จีโนมเสถียรนั้นเซลล์จะมีกระบวนการควบคุมเหนือพันธุกรรมเพื่อลดความตึงเครียดของสายดีเอ็นเอเพื่อไม่ให้เกิดการทำลายดีเอ็นเอ สภาวะเหนือพันธุกรรมนั้นเรียกว่า การฉีกขาดของดีเอ็นเอสายคู่แบบที่เกิดขึ้นเองที่สามารถพบในระยะที่เซลล์ไม่แบ่งตัว (RIND-EDSBs) หรือข้อต่อดีเอ็นเอ (Youth-DNA-GAPs) ข้อต่อดีเอ็นเอนี้จะอยู่ในบริเวณที่มีเมทิลเลชันของจีโนมและถูกรักษาไว้ด้วยโปรตีน HMGB1 และ โปรตีน SIRT1 การที่ระดับเมทิลเลชันของทั้งจีโนมลดลงจะส่งผลให้ข้อต่อดีเอ็นเอลดลงซึ่งสามารถพบได้ในเซลล์มะเร็งและเซลล์แก่ ดังนั้นการศึกษาครั้งนี้จึงมีวัตถุประสงค์ในการศึกษาบทบาทของโปรตีน HMGB1 ซึ่งเป็นตัวกลางของกระบวนการเมทิลเลชันในการป้องการความไม่เสถียรของจีโนม ประการแรกจากการศึกษาโดยใช้เทคนิค IRS-EDSB LMPCR และ DI-PLA พบว่าบริเวณ Box-A domain ของโปรตีน HMGB1 เป็นตัวสร้างข้อต่อดีเอ็นเอ ประการที่สองผลจากการทดสอบด้วยเทคนิค PLA พบว่าโปรตีน HMGB1 สร้าง complex กับข้อต่อดีเอ็นเอ (Youth-DNA-GAPs) และโปรตีน SIRT1 นอกจากนี้ยังพบว่าโปรตีน SIRT1 ทำหน้าที่ป้องกันข้อต่อดีเอ็นเอจาก γ H2AX ประการที่สาม ผู้วิจัยได้คิดค้นวิธี PCR ใหม่ 2 วิธีเพื่อใช้ในการศึกษาการกระจายตัวของข้อต่อดีเอ็นเอในจีโนม ได้แก่วิธี DNA immunoprecipitate 8-OHdG และวิธี IRS-SSB PCR ร่วมกับ EDSB-SSB PCR จากการศึกษาพบว่าข้อต่อดีเอ็นเออยู่ห่างจากดีเอ็นเอที่ถูกทำลายชนิดต่างๆ และสามารถทำให้จีโนมเสถียรเป็นบริเวณกว้าง ประการสุดท้ายคือการศึกษากลไกของโปรตีน HMGB1 ว่าเป็นตัวกลางของกระบวนการดีเอ็นเอเมทิลเลชัน โดยทำการใส่ Alu siRNA และ AGO4 ไปในเซลล์มนุษย์ ผลการศึกษาพบว่าโปรตีน HMGB1 และกระบวนการดีเอ็นเอเมทิลเลชันมีความสัมพันธ์ซึ่งกันและกันในการช่วยป้องกันความไม่เสถียรของจีโนม

จุฬาลงกรณ์มหาวิทยาลัย
CHULALONGKORN UNIVERSITY

สาขาวิชา ชีวเวชศาสตร์ ลายมือชื่อนิสิต .....

ปีการศึกษา 2563 ลายมือชื่อ อ.ที่ปรึกษาหลัก .....

5887786120 : MAJOR BIOMEDICAL SCIENCES

KEYWORD: HMGB1 RIND-EDSB Youth-DNA-GAP DNA methylation Genomic instability

Papitchaya Watcharanurak : High-mobility group box 1 (HMGB1) mediates DNA methylation preventing genomic instability. Advisor: Prof. Dr. APIWAT MUTIRANGURA, M.D., Ph.D.

Global DNA hypomethylation promotes genomic instability through the accumulation of DNA damage and resulted in an increasing rate of mutation. To stabilize the genome, cells possess an epigenetic mechanism to reduce DNA tension that causes DNA damages, named Replication-Independent Endogenous DNA Double-Strand Breaks (RIND-EDSBs). Due to their biological roles, this type of physiologic EDSBs act as youth-associated genomic-stabilizing DNA gaps (Youth-DNA-GAPs). They are localized within methylated genome and maintained by non-histone HMGB1 and SIRT1 proteins. Reduction of RIND-EDSBs was found in hypomethylated genome, including cancer and aging. Therefore, this study aimed to explore the role of HMGB1-mediated DNA methylation in genomic instability prevention. First, using IRS-EDSB LMPCR and DI-PLA methods, we demonstrated that HMGB1, specifically Box-A domain produces Youth-DNA-GAPs. Second, the results from PLA assay revealed that HMGB1 forms complex with Youth-DNA-GAPs and SIRT1, and SIRT1 protected Youth-DNA-GAPs from γ H2AX. Third, we conducted two novel PCR, DNA immunoprecipitate 8-OHdG followed by IRS-EDSB LMPCR and IRS-SSB PCR combined with EDSB-SSB PCR to study genome distribution pattern of Youth-DNA-GAPs, and found that Youth-DNA-GAPs are located far from DNA damages and can stabilize genome in long distance. Finally, to study the mechanism of HMGB1-mediated DNA methylation, Alu siRNA and AGO4 transfection were performed. We showed that DNA methylation preventing genomic instability is HMGB1 dependent. Therefore, HMGB1 mediates DNA methylation by producing and maintaining methylated RIND-EDSB or Youth-DNA-GAPs in methylated genome to prevent genomic instability.

จุฬาลงกรณ์มหาวิทยาลัย
Chulalongkorn University

Field of Study:	Biomedical Sciences	Student's Signature .....
Academic Year:	2020	Advisor's Signature .....

ACKNOWLEDGEMENTS

I am sincerely grateful to all of the people who provided help in many ways to make my doctoral dissertation possible.

First of all, I would like to express my sincere gratitude to my advisor, Professor Dr. Apiwat Mutirangura. I feel really lucky to have an advisor who's always there whenever you need help. I am very grateful for his continuous encouragement and support, patience, motivation, advice and expertise.

I am also thankful to Dr. Narumol Bhummaphan, Dr. Charoenchai Puttipanyalears, Dr. Kanwalat Chalerphet, and Dr. Maturadara Patchsung for their help in experimental, ideas and insightful comments.

Further thanks to my members in AM lab. It has been a great and enjoyable experience working with them, and I am gratified for their help and encouragement.

Finally, my special thanks go to my family for their unconditional love, supports, motivation, and for always stand by my side.

This thesis was supported by the Chulalongkorn University 100th Anniversary Doctoral Degree Scholarship and 2019 Research Chair Grant from the National Science and Technology Development Agency, Thailand.

จุฬาลงกรณ์มหาวิทยาลัย
CHULALONGKORN UNIVERSITY

Papitchaya Watcharanurak

TABLE OF CONTENTS

Page

ABSTRACT (THAI) iii

ABSTRACT (ENGLISH) iv

ACKNOWLEDGEMENTS v

TABLE OF CONTENTS vi

LIST OF TABLES vii

LIST OF FIGURES viii

CHAPTER I INTRODUCTION 1

CHAPTER II LITERATURE REVIEW 6

CHAPTER III MATERIALS AND METHODS 16

CHAPTER IV RESULTS 25

CHAPTER V DISCUSSION 50

REFERENCES 57

VITA 65

จุฬาลงกรณ์มหาวิทยาลัย
CHULALONGKORN UNIVERSITY

LIST OF TABLES

Page

Table 1. DI-PLA and PLA antibodies used in this study 24

จุฬาลงกรณ์มหาวิทยาลัย
CHULALONGKORN UNIVERSITY

LIST OF FIGURES

Page

Figure 1. The structure of HMGB1 protein 7

Figure 2. The function of HMGB1 protein 8

Figure 3. Levels of RIND-EDSBs in human (A) and yeast (B). 10

Figure 4. The characteristics of RIND-EDSBs detected in human cells. 10

Figure 5. Levels of RIND-EDSBs in yeast strains with deletions of genes encoding proteins with the High-Mobility Group B (HMGB) (A) and topoisomerase and endonuclease (B). 11

Figure 6. Schematic of canonical and non-canonical RdDM pathway. 14

Figure 7. HEK293 cells express GFP after transduction with viral particle containing shRNA. 25

Figure 8. Lentivirus-mediated HMGB1- and SIRT1-shRNA knockdown of HEK293. 26

Figure 9. Real-time RT-PCR and western blot analysis confirmed the expression of HMGB1 stable knockdown cells. 27

Figure 10. Real-time RT-PCR and western blot analysis confirmed the expression of SIRT1 stable knockdown cells. 28

Figure 11. The levels of Youth-DNA-GAPs in HMGB1 knockdown. 29

Figure 12. Co-localization of Box A and Youth-DNA-GAP by DI-PLA assay. 31

Figure 13. Detection of Box-A and γH2AX colocalization after TSA treatment by PLA assay. 33

Figure 14. Colocalization staining of proteins from Box-A plasmid transfection and γH2AX. 34

Figure 15. Colocalization of Youth DNA-GAPs and SIRT1 detected by DI-PLA. 35

จุฬาลงกรณ์มหาวิทยาลัย
Chulalongkorn University

Figure 16. Box-A of HMGB1 interacts with SIRT1. 36

Figure 17. DNA-GAP PCR of DIP 8-OHdG PCR vs total genomic DNA..... 37

Figure 18. The comparison of IRS-SSB PCR and EDSB-SSB PCR. 38

Figure 19. Levels of Alu methylation located near EDSBs in HMGB1 knocked down cells..... 40

Figure 20. Downregulation of HMGB1 reduces genomic Alu methylation levels. 40

Figure 21. Overexpression of HMGB1 increases genomic Alu methylation levels..... 41

Figure 22. Alu methylation level upon Alu siRNA transfection in HMGB1 knockdown cells..... 43

Figure 23. Alu methylation level upon AGO4 transfection in HMGB1 knockdown cells. 44

Figure 24. The interaction between AGO4 and HMGB1 protein by proximity ligation assay. 46

Figure 25. Cell viability of Alu siRNA transfection under stably knockdown of HMGB1. 47

Figure 26. Detection of γH2AX by western blot analysis in (A) siAlu and lipofectamine transfection in HEK293 for 48 h and (B) AGO4 and PC transfected HEK293 cells at 72h. 48

Figure 27. Immunoblot of γH2AX in siAlu- and AGO4-transfected cell upon HMGB1 knockdown. 49

Figure 28. Schematic representation two hypotheses of how HMGB1 mediates DNA methylation preventing genomic instability..... 55

จุฬาลงกรณ์มหาวิทยาลัย
Chulalongkorn University

CHAPTER I
INTRODUCTION

Background and rationale

Loss of intersperse repetitive sequence (IRS) methylation or global hypomethylation is a common characteristic driving aging process (1) and carcinogenesis (2). Genome-wide hypomethylation leads to genomic instability through the accumulation of DNA damage and resulted in an increasing rate of mutation (3). Therefore, DNA methylation in IRS is essential for the maintenance of genome stability which is crucial for proper functions and survival of the cells. Human genome is composed of more than 50 % of IRS, and over 90% of methylated CpG sites occur in IRS. Alu and LINE-1 are represented as two major types of long interspersed nuclear elements (LINE) and short interspersed nuclear elements (SINE), respectively (4). Thus, decreased DNA methylation in these IRS can be referred as global DNA methylation (5-7). The function of IRS DNA methylation is responsible for control gene expression and prevent genomic instability (8-9). Among IRS methylation, decreased Alu methylation is the most representative of genome-wide hypomethylation, driving genomic instability (3). Therefore, our study focus on the alteration of methylation in Alu repetitive sequences which is the most suitable target for a genomic instability study.

จุฬาลงกรณ์มหาวิทยาลัย
Chulalongkorn University

Because DNA methylation is commonly found on transposons and other repetitive DNA elements (10-11), to preserve genome stability, cells possess a mechanism to control DNA methylation by which small interfering RNA can direct methylate DNA, named RNA-directed DNA methylation (RdDM). RdDM machinery facilitates genome stability by transcriptional silencing of repetitive sequences. RdDM is a biological process in which small non-coding RNAs are colocalized with AGO4 protein and the complex can directly de novo methylation at specific DNA sequences by recruiting domains rearranged 2 (DRM2) de novo methyltransferase. To de novo methylate at its target loci, the RdDM process requires several proteins involved in siRNA production, histone modification,

chromatin remodelling, and DNA methylation (12-15). Our previous works have been identified RdDM in human cells. AGO4 was an effector proteins in human RdDM, and preferentially bound to repetitive sequences, LINE-1 and Alu (16). Alu siRNA promoted Alu methylation and resulted in DNA lesion reduction (17). However, the mechanism by which DNA methylation can prevent DNA damage has not been known.

Within the methylated genome, the existence of physiologic endogenous DNA double strand breaks (EDSBs) has been detected. A decade ago, our lab discovered another type of EDSBs, Replication Independent EDSBs (RIND-EDSBs) which can be found without the influence of DNA replication (18). RIND-EDSBs are evolutionally conserved and ubiquitous presented in the G0 phase of the cell cycle. These physiologic EDSBs have different characteristics from replication or radiation-induced EDSBs. While pathologic EDSBs halt the cell cycle and lead to cell death, physiologic RIND-EDSBs act differently (19-20). The molecular mechanism of RIND-EDSBs has been investigated in yeast strains mutant genes in several cellular pathways. The number of RIND-EDSBs was lower in yeast strains lacking HMGB protein and Sir2, suggesting that HMGB and Sir2 may play a role in maintaining RIND-EDSBs. Whereas the number of RIND-EDSBs was higher in yeast strains with gene deletion of endonucleases and topoisomerase, indicating a compensatory mechanism of RIND-EDSBs (19). RIND-EDSBs occur nonrandomly and are maintained in the specific location of genome. They frequently appeared after “ACGT” sequence (21). Importantly, DNA methylation typically occurred at CpG sites. This might be the reason why physiologic RIND-EDSB have “ACGT” pattern. In human, RIND-EDSBs are localized in hypermethylated region of genome, preferentially retained within heterochromatin, and not related to *γH2AX which is a critical DSB response* (20). Notably, physiologic RIND-EDSBs are reduced in aging yeast, and low levels of RIND-EDSBs result in decreased cell viability and increased DNA damage. According to their biological role, we renamed them to youth-associated genome-stabilizing DNA gaps (Youth-DNA-GAPs) (22).

Because physiologic RIND-EDSBs are localized in hypermethylated genome, a decrease in genome-wide methylation results in low levels of physiologic RIND-EDSBs

(18). Furthermore, global hypomethylation induces genomic instability. Therefore, we hypothesized that RIND-EDSBs are kept in hypermethylated regions to prevent genomic instability which is a precursor driving aging and cancer. Moreover, RIND-EDSBs play a role redundant to topoisomerase II which can induce EDSBs to relieve DNA stress during transcription and replication (19). Therefore, the accumulation of RIND-EDSBs in hypermethylated genome may play an epigenetic role in reducing DNA tension similar to the gap of railway track.

As described previously, physiologic RIND-EDSBs were reduced in yeast strains lacking HMGB protein and Sir2. So, this means that physiologic RIND-EDSBs are produced or maintained with specific proteins. High-mobility group box 1 (HMGB1), abundant non-histone proteins in nucleus serves as the structural protein of chromatin that can bind and bend DNA. HMGB1 facilitates nuclear homeostasis and genome stability by implicated in multiple DNA-dependent processes including, DNA replication, transcription, recombination, and DNA repair (23-24). Moreover, several lines of evidences supported the function of HMGB1 that can be associated with physiologic RIND-EDSBs. HMGB1 participates in the V(D)J cleavage reaction, another type of physiologic EDSBs (26). It has a weak 5'-deoxyribose phosphate lyase activity that can cut DNA (27). Interestingly, HMGB1 and HMG box A possess nuclease activity (Chalerphet K, unpublished data). In addition, the role of HMGB1 on genomic stability maintenance in eukaryotic cells have been identified. HMGB1 in mammalian and its homolog (nhp6a/b) in yeast can protect DNA from damaging agents which result in the reduction of genomic aberrations (28). Our previous study showed that down-regulation or deletion of high mobility group genes in both humans and yeasts have a higher level of endogenous DNA damages, including 8-OHdG and AP-site. In addition, our preliminary study also elucidated that not only HMGB1 possesses a role in reducing genomic instability, but Box A of HMGB1 also play a potential role in this phenomenon (Settayanon S, unpublished data). Sir2, homologue of human SIRT1 is a histone deacetylase that mediates heterochromatin formation. It is well known that SIRT1 is associated with aging process, and reduction of SIRT1 caused increased DNA damages (29-30).

Because methylated RIND-EDSBs (Youth-DNA-GAPs) are maintained by HMGB1 and the functions of HMGB1, RIND-EDSBs, and genome-wide methylation are against genomic instability, the connection among three epigenetic candidates needs to be elucidated. Therefore, the main objective of this study is to explore the role of HMGB1 in mediating DNA methylation to prevent genomic instability. These findings could be necessary for a better understanding of how DNA methylation can prevent genomic instability.

Research questions

1. Does HMGB1 produce RIND-EDSBs or Youth-DNA-GAPs ?
2. Does HMGB1 form complex with SIRT1 and RIND-EDSBs or Youth-DNA-GAPs ?
3. Does the complex prevent genomic instability?
4. How is the role of HMGB1-mediated DNA methylation preventing genomic instability?

Hypotheses

1. HMGB1 produces RIND-EDSBs or Youth-DNA-GAPs.
2. HMGB1 forms complex with SIRT1 and Youth-DNA-GAPs.
3. If Youth-DNA-GAP is a stabilizing epigenetic mark, it should be far from DNA damage.
4. If HMGB1 is a mediator that connect between methylated RIND-EDSBs (Youth DNA GAPs) and DNA methylation, genomic instability prevention by DNA methylation will not occur when HMGB1 is inhibited.

NGKORN UNIVERSITY

Objectives

1. To test whether HMGB1 generates Youth-DNA GAPs.
2. To examine whether HMGB1 form Youth-DNA GAPs complex in methylated genome.
3. To investigate whether Youth-DNA-GAPs produced by HMGB1 can prevent genomic instability by observe genome distribution pattern.
4. To clarify whether HMGB1 mediates DNA methylation to prevent genomic instability.

Conceptual Framework

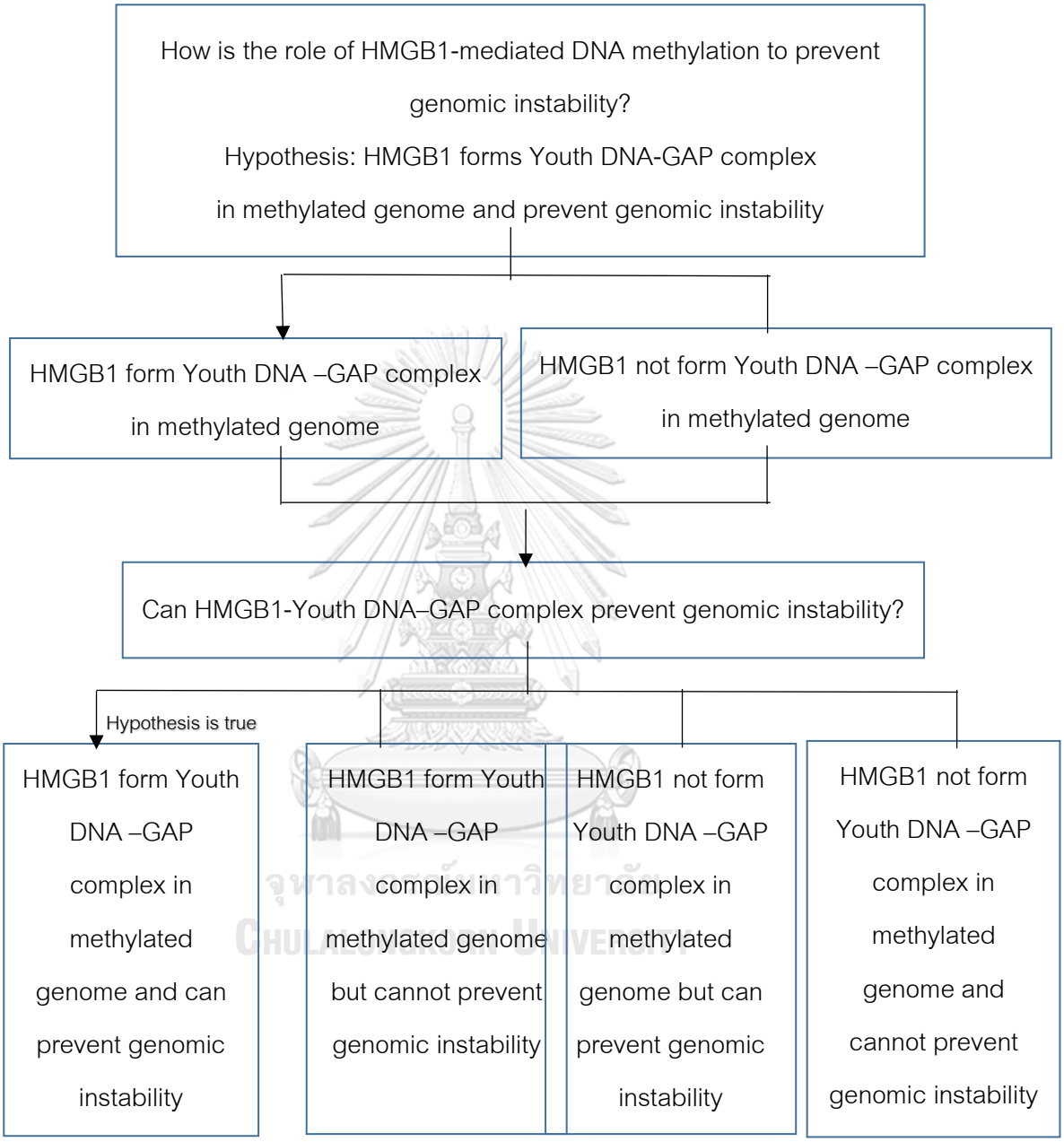

CHAPTER II
LITERATURE REVIEW

High mobility group box 1 (HMGB1)

High mobility group box 1 (HMGB1 or HMG-1 or amphoterin) is an evolutionarily conserved non-histone architectural proteins belonging to the high-mobility group *(*HMG*)* protein superfamily. It was first identified in calf thymus in 1973 and is named according to its electrophoretic mobility on polyacrylamide gels (31). In mammal, the HMGB protein family can be subdivided into four subfamily: HMGB1, HMGB2, HMGB3, and HMGB4. HMGB1 are highly abundant and ubiquitously expressed in most mammalian cells, except cells that have no nucleus such as erythrocytes and cornifying epithelial cells (32).

In human, HMGB1 gene is located on chromosome 13q12 and comprises of five exons. HMGB1 consists of 215 amino acid residues and has a molecular weight of ~25 (27-32) kDa protein. The structure of HMGB1 includes of three functional domains: two DNA-binding HMG-box domains (N-terminal Box A and central Box B) which have positively charged, residues 1–79 and 89–163, respectively, and an acidic C terminal tail which has negatively charged, residues 186–215 (Figure 1) (33-34). This structure provide form of HMGB1 to recognize and specifically bind DNA structures, containing bends or kinks DNA (35-36). The A and B boxes are two homologous DNA-binding motifs that can bind to DNA without sequence specificity. It has been reported that B box can mediates pro-inflammatory activity which residues 150- 183 are responsible for binding with receptor for advanced glycation end products (RAGE), while residues 89-108 are responsible for binding with Toll-like receptors (TLRs) (37). By contrast, the A box acts as

a specific antagonist of full length HMGB1 (36). Moreover, the C-terminal acidic tail plays an important role in nuclear functions and helps HMGB1 DNA-binding specificity (37).

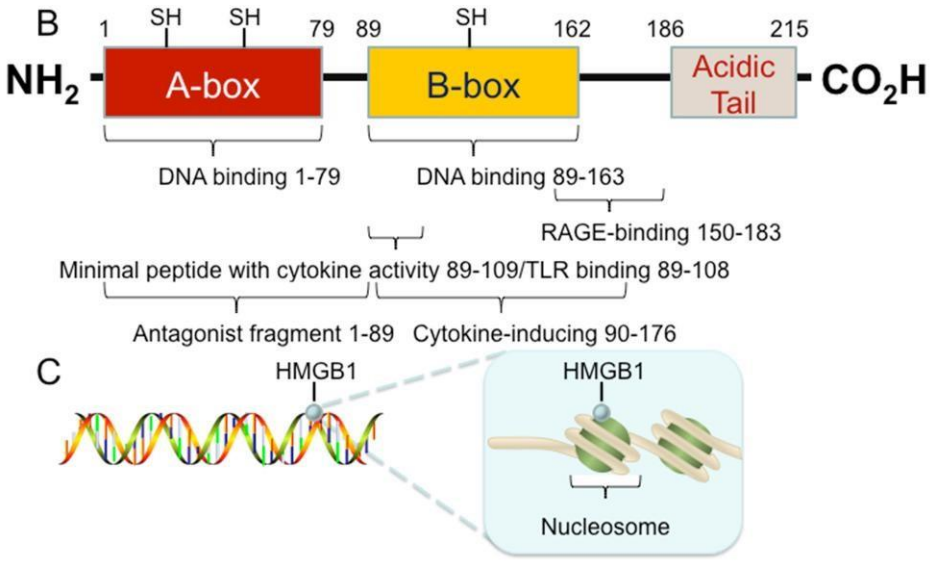

Figure 1. The structure of HMGB1 protein (30).

HMGB1 can shuttle between nucleus and cytoplasm; therefore, the role of HMGB1 is depended on its location via acetylation process. Apart from nuclear localization, HMGB1 can be located in cytoplasm, cell surface membranes, and extracellular space. HMGB1 is a multifunctional protein which is involved in a variety of cellular biological processes (Figure 2) (39, 41). In the nucleus, HMGB1 function as a DNA chaperone that can bind to the minor groove of DNA and bend it into a helical structure, and also change the conformation of DNA (40). HMGB1 stabilizes nucleosomes and participates DNA replication, gene transcription, V(D)J recombination, and DNA repair. Thus, nuclear HMGB1 serves an important role in maintaining nuclear homeostasis and stability. In cytoplasm, HMGB1 is involved in immune responses by inhibiting apoptosis, increasing autophagy, and regulating mitochondrial function. Extracellular HMGB1 functions as a cytokine that can activate the immune response, and implicated in the regulation of inflammation and cancer progression (32, 37-40).

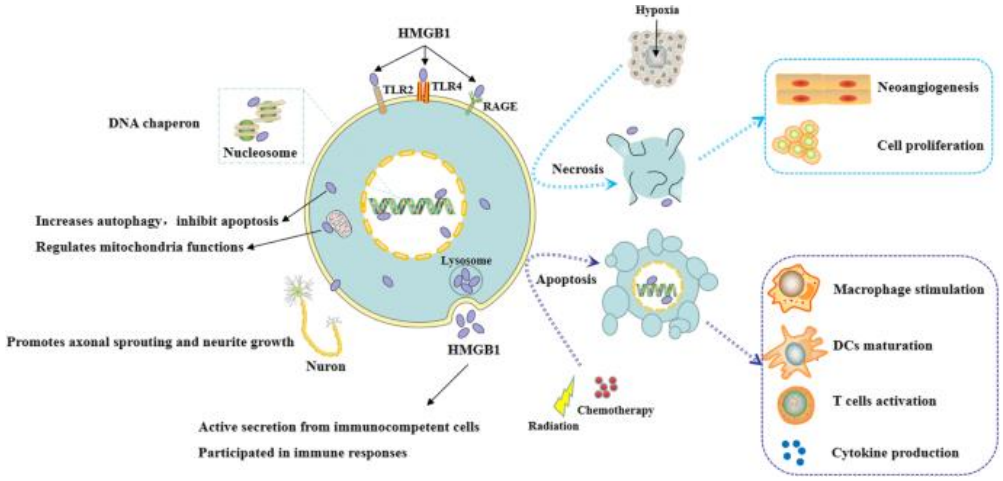

Figure 2. The function of HMGB1 protein (41).

The roles of HMGB1 on genome instability protection

Many researchers have demonstrated the role of HMGB1 in modulating genome stability. Loss of HMGB1 in cells displays telomere shortening by which telomere is essential for chromosome stability (43). Moreover, there is an evidence showed that HMGB1 in mammalian and Nhp6A/B; HMGB1 homolog in yeast have ability to protect DNA from damaging agents resulted in against the generation of genomic aberrations (44). Recently, results from our experiment also revealed the potential role of HMGB1 especially, HMG A box (Box A) of HMGB1 in preventing genomic instability. In HMGB1 and Box A overexpression, cells exhibited lower levels of endogenous DNA damage; AP-site and 8-OHdG and cell viability of overexpressed cells was increased after exposed to DNA damaging agents; H_2O_2 and rapamycin (Patchsang M. and Settayanon S, unpublished data). Moreover, HMGB1 has been identified to prevent genomic instability by retaining physiologic RIND-EDSBs. Levels of RIND-EDSBs were decreased in yeast cell lacking Nhp6A/B genes and the similar result has been observed in HeLa cells downregulated HMGB1 (19). Taken together, these findings suggest that HMGB1 retains these physiologic EDSBs and these EDSBs type might serve for specific function in maintaining genome stability. However, the mechanism of HMGB1 proteins in producing or retaining RIND-EDSBs will be further investigated. In addition, there are several lines of evidences supported the function of HMGB1 that can be associated with physiologic

RIND-EDSBs. HMGB1 participates in the V(D)J cleavage reaction, another type of physiologic EDSBs (25). It has a weak 5'-deoxyribose phosphate lyase activity that can cut DNA (27). Interestingly, HMGB1 and HMG box A possess nuclease activity (Chalerphet K, unpublished data). Interestingly, It has been reported that Box-A domain of HMGB1 interact with SIRT1, a nicotinamide dinucleotide (NAD+)-dependent histone deacetylase that mediates heterochromatin formation. SIRT1 is associated with aging process, and reduction of SIRT1 caused increased of DNA damages (29-30).

Replication-independent endogenous double-strand breaks (RIND-EDSBs)

DNA double strand breaks (DSBs) are a most severe type of DNA damage, therefore, unrepaired DSBs can contribute to genomic instability leading to deterioration aging and carcinogenesis (45). DSBs are caused by exogenous exposure to radiation and chemicals, and they can occur endogenously by metabolic processes such as mechanical stress and DNA replication through single stranded lesions (46) However, some endogenous DNA double strand breaks are generated by physiologic processes as programmed DSBs. For example, RAG protein complex produces DSBs in V(D)J recombination process which is essential for assembling of immunoglobulin antigen receptor genes, as well as T-cell receptor genes in lymphocytes, and topoisomerase II generates DSB to relieve DNA tension during transcription and replication (47)

จุฬาลงกรณ์มหาวิทยาลัย
CHULALONGKORN UNIVERSITY

In 2008, our lab discovered new type of endogenous DNA double strand breaks that occur without the effect DNA replication. They can be detected at G0 phase or resting state of cell cycle, namely "Replication-INDependent EDSBs" (RIND-EDSBs). RIND-EDSBs are evolutionally conserved from yeast to human (Figure 3) (18-19). The causes and consequences of RIND-EDSBs are differently from pathologic EDSBs; replication-dependent EDSBs and environmental- or radiation-induced EDSBs (20). Recently, it has been proved that physiological RIND-EDSBs play an epigenetic role in preventing pathological RIND-EDSBs, a type of DNA damage in chronologically aging cells (48).

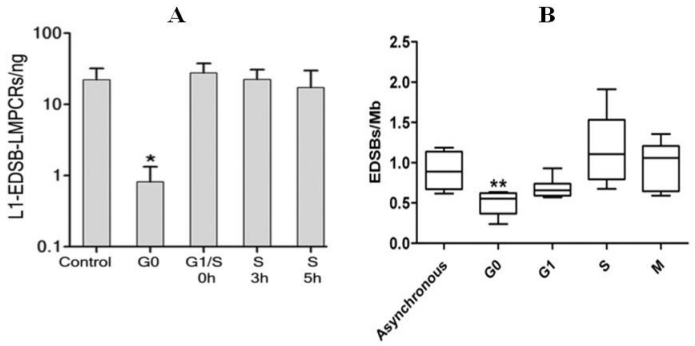

Figure 3. Levels of RIND-EDSBs in human (A) and yeast (B). RIND-EDSB are evolutionally conserved from yeast to human. RIND-EDSB can be found in all phase of cell cycle, including G0 phase.

In human, RIND-EDSBs are presented in all cell types including normal and cancer (18). The characteristics of RIND-EDSBs detected in human cells are localized in hypermethylated genome, preferentially retained within heterochromatin, unbound by γH2AX, the earliest signal of double strand breaks, and repaired by precise ataxia telangiectasia mutated (ATM)-dependent non-homologous end-joining pathway (NHEJ). In contrast, pathologic EDSBs are commonly localized in hypomethylated genome, retained in the euchromatin, bound by γ-H2AX, and repaired by faster, more-error prone Ku-mediated NHEJ (Figure 4) (20).

จุฬาลงกรณ์มหาวิทยาลัย

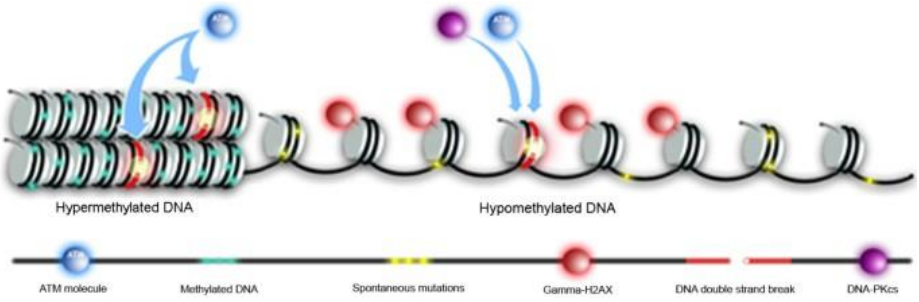

Figure 4. The characteristics of RIND-EDSBs detected in human cells. Under normal physiological conditions, RIND-EDSBs are hypermethylated, retained in heterochromatin and preferentially repaired by different pathways to pathologic EDSB.

In yeast, RIND-EDSBs were scattered along chromosomes and the number of breaks correlated with chromosomal size. The breaks had specific pattern of sequences. Most of the breaks occurred after the sequence “ACGT”. This observation indicated that RIND-EDSB production is regulated by a non-random mechanism (21). Moreover, the levels of RIND-EDSBs in yeast *Saccharomyces cerevisiae* lacking genes in several cellular pathways have been observed to clarify molecular mechanism. The number of RIND-EDSBs was lower in yeast strains which deleted of the HMGB protein and Sir2, suggesting that HMGB1 and Sir2 may play a role in maintaining RIND-EDSBs. In contrast, the number of RIND-EDSBs was higher in yeast strains with lacking of endonucleases and topoisomerase, this data suggesting the role in compensatory mechanism of RIND-EDSBs (Figure 5) (19).

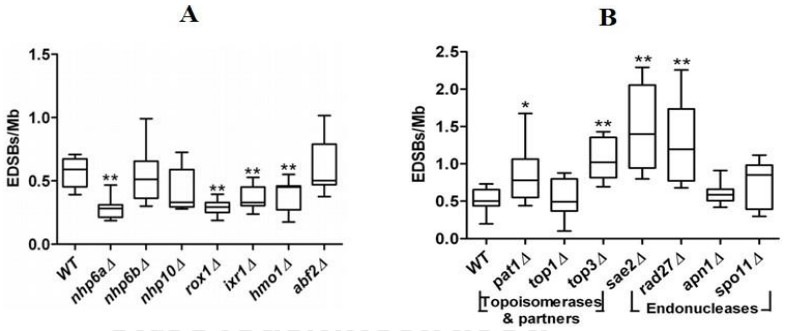

Figure 5. Levels of RIND-EDSBs in yeast strains with deletions of genes encoding proteins with the High-Mobility Group B (HMGB) (A) and topoisomerase and endonuclease (B).

จุฬาลงกรณ์มหาวิทยาลัย
Chulalongkorn University

Global hypomethylation and Genomic instability

DNA methylation is an epigenetic modification that allows heterochromatin formation and gene silencing. It is the mechanism by which the methyl (CH3) group are add to the carbon 5 position of the cytosine ring by enzyme DNA methylatransferase (DNMTs). DNMT1 is responsible for maintenance methylation, as it preferentially methylates hemimethylated substrates, whereas DNMT3a and -3b are defined as *de novo* methylases for their ability to methylate unmethylated DNA. DNA methylation can

occur in many location of the genome, such as intergenic region, repetitive sequence and CpG Island. The fundamental roles of DNA methylation are controlling gene expression and preserving genome stability. DNA methylation is an essential epigenetic mechanism for silencing transposons and other interspersed repetitive sequences (49-51).

Throughout the human genome, DNA repetitive elements encompass account for about 50% of the genome (52). They can replicate and insert copies of themselves at other locations within a host genome. The two most abundance of IRS include Alu element (Alu) and long interspersed element-1 (LINE-1), with approximately 1 million Alu repetitive elements and half a million LINE-1 elements interspersed throughout the human genome (53, 55). Alu and LINE-can insert target protein-coding genes which may cause genomic instability and contribute to the development of human diseases, including cancer (3, 56-59). Reduction of DNA methylation in IRS, widely referred as global hypomethylation. Over 90% of methylated CpG sites in the human genome occur in IRS, particularly Alu and LINE-1 (52). Therefore given their genome-wide ubiquity and CpG rich content, an assessment of methylation in Alu and/or LINE-1 methylation have been widely used as surrogate measures of global DNA methylation in several studies in human. The levels of global methylation have been studied in many types of IRS, including LINE-1, HERVs, and Alu. However, decrease in methylation at Alu repeat represents a global hypomethylation causing genomic instability more than others (60-61).

จุฬาลงกรณ์มหาวิทยาลัย
Chulalongkorn University

Several lines of evidences suggest that DNA methylation plays a role in maintaining genomic instability. Global hypomethylation commonly occurs in both cancer aging (56-60), which leads to higher rates of mutations and genomic instability. Genomic instability is the imbalance between DNA damages formation and DNA repair resulted in high frequency rate of mutations (62-63). Molecular mechanism underlying genomic instability are DNA double strand breaks (DSBs) and DSB repair (64). In our previous study, we have shown that in non-replicative cells, there are two types of Endogenous DNA Double strand break (EDSBs). First is pathologic DNA lesions or pathologic-EDSBs. Pathologic-EDSBs, like the replication or irradiation induced DSBs, lead to mutations and cause cell death (48).

RNA-directed DNA methylation (RdDM)

RNA-mediated transcriptional gene silencing (RNAi) is fundamental biological process in which double-stranded RNA can suppress gene expression through translation or transcriptional repression. One mechanism of RNAi is RNA-directed DNA methylation (RdDM). RdDM machinery which was first discovered in tobacco plants (65) is a mechanism in which noncoding RNA direct addition of DNA methylation to specific DNA sequences. RdDM play a role to in several biological process, including transcriptional repression, pathogen defense, and maintenance of genome stability by suppression transposon activity (66). AGONAUTE (AGO) protein is an effector protein in RNAi pathway. However, the function of AGO4 has been extensively studied in RdDM (67-68). In plants, the RdDM process is starts with the biogenesis of 24-nucleotide siRNAs from target loci then single guide RNA are load onto AGO4 protein. siRNA-AGO4 complex recruit domains rearranged 2 (DRM2) de novo methyltransferase to facilitate target methylation. RdDM can be divided into 2 pathways: canonical and non-canonical RdDM pathway depending on a specialized transcriptional process which involves different types of size of sgRNA, RNA polymerase, and effector proteins such as AGO protein (Figure 6) (65-70).

จุฬาลงกรณ์มหาวิทยาลัย
Chulalongkorn University

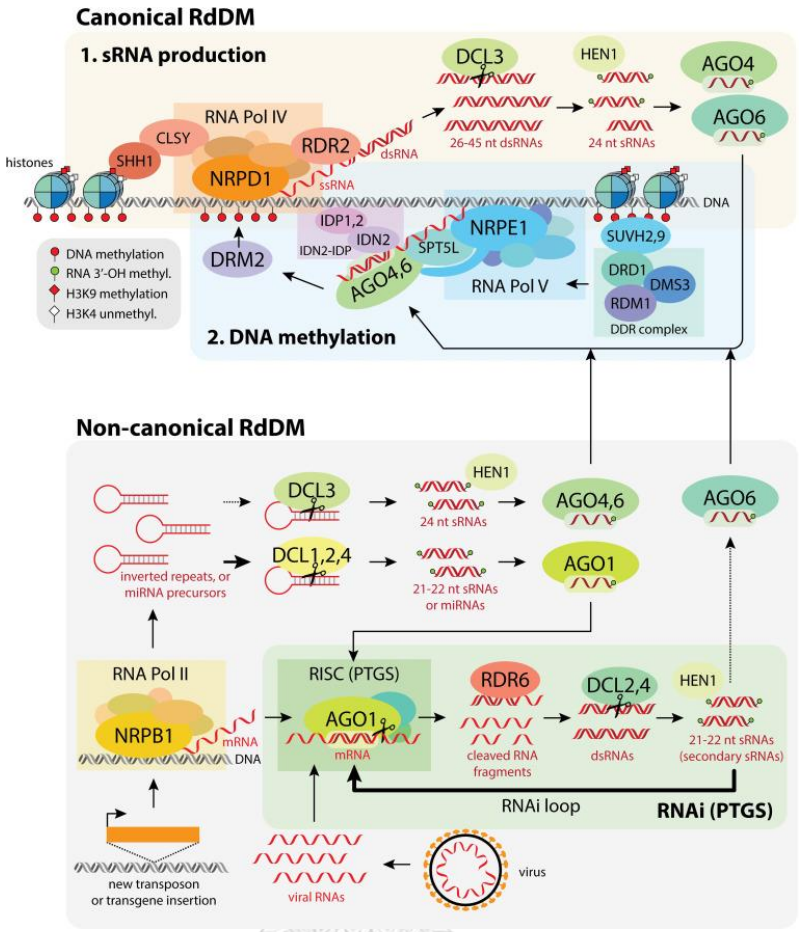

Figure 6. Schematic of canonical and non-canonical RdDM pathway. Canonical pathway (top) consists of the biogenesis of siRNA which is processed by Pol IV, RDR2 and DCL3 and loading of 24-nt siRNAs into AGO4 or AGO6 then scaffold RNA production is processed by Pol V and protein recruitment for DNA methylation is processed by DRM2. Non-canonical pathway (bottom) is involved in biogenesis of siRNA which is processed by Pol II, RDR6 and DCL2 or DCL4 and loading of 21-nt siRNAs into AGO1 and cleavage of mRNA (RNAi). However, some of 21-nt siRNA can be loaded onto AGO6 (66).

Although RdDM is well documented in plant, a potentially related process of RNA-directed has been explored in human both in specific gene and repetitive sequences (16-17, 71-72). RASSF1A shRNA *de novo* methylates at

RASSF1A promoter in HeLA cell. Alu siRNA transfection could promote Alu methylation (17). Moreover, AGO4 incorporate with single guide RNA of Alu augmented Alu methylation in HeLa cell lines (16). In addition, antisense transcripts of L1 can inhibit L1 retrotransposition through DNA methylation (71).

จุฬาลงกรณ์มหาวิทยาลัย
Chulalongkorn University

CHAPTER III
MATERIALS AND METHODS

Cell culture

HEK293 and HK2 cells were obtained from American Type Culture Collection. Cell were cultured in Dulbecco's Modified Eagle Medium (DMEM) (Gibco), supplemented with 10% fetal bovine serum (FBS) and 1% antibiotic-antimycotic maintained in humidified atmosphere at 37 ^{o}C with 5% CO_2.

Plasmid construction and production

For HMGB1 overexpression, a full-length human HMGB1 and plasmid control (pcDNA 3.1) were purchased from Addgene (MA, USA). The Box A, Box A mutant (p.Phe38Tyr, p.Phe38Trp and p.Phe38Gly), Box-B, and Box BC were constructed by GeneArt Gene synthesis (Thermo Fisher). In addition, pIRESneo-FLAG/HA AGO4 and FLAG-HA-pcDNA3.1 empty vector were purchased from Addgene (MA, USA) and used for AGO4 overexpression experiment. To produce plasmid, each plasmid was transformed into Escherichia coli (DH5α); NEB® 5-alpha competent E.coli (New England BioLabs). For plasmid selection, E.coli (DH5α) with plasmid expression vector contains neomycin resistant gene, were grown on LB agar with ampicillin following culture the selected colony in LB broth with 100 µg/ml of ampicillin and incubated on incubator shaker at 37 ^{o}C for 16 h. Isolation of plasmid DNA was performed using GeneJET Plasmid Miniprep Kit (Thermo Scientific).

จุฬาลงกรณ์มหาวิทยาลัย
CHULALONGKORN UNIVERSITY

Plasmid Transfection

The day before transfection, cells were seeded at 3 × 10^5 cells per well in 6-well plate in 2 ml DMEM containing 10% FBS. Then 2500 ng (HMGB1 plasmid) or 2000 ng (AGO4 plasmid) was transfected using Lipofectamine® 3000 (Invitrogen) following to the manufacturer's protocols.

Generation of shHMGB1 knocked-down HEK293 cell lines

To generate stable cell knockdown cells, HMGB1 shRNA vector (shHMGB1) (cat.no: TL316576) or SIRT1 shRNA vector (shSIRT1) (cat.no: TL309433), and scrambled pGFP-C-shLenti shRNA negative control (shScramble) (cat.no: TR30021) were purchased from Origene (Rockville, MD, USA). Production of viruses was carried out by co-transfection of HEK293T cells (2.5×10^5 cells) with 500 ng vectors containing shRNA vectors and 600 ng packaging plasmid (Lentivpak packaging kit; cat. no. TR30037) using Turbofectin transfection reagent (OriGene Technologies, Inc.). After transfection for 48 h and 72 h, the supernatant containing viral particles was subsequently collected and filtered through a filter with a pore size of 0.2–0.45 μm. Lentiviral particle containing HMGB1 shRNA (shHMGB1), SIRT1 shRNA (shSIRT1) or negative control shRNA (shScramble) were transducted into HEK293 cells with MOI of 5 in culture medium containing 8 μg/ml polybrene (Sigma-Aldrich). After 24 h post transduction, the medium was remove and fresh medium was added. Then, cell were continued cultured in the presence of 1 ug/ml puromycin for 2-4 weeks.

shRNA transient transfection

Lipofectamine® 3000 (Invitrogen MA, USA) was used for transient transfection according to the manufacturers' protocols. Briefly, HEK293 cells were seeded into a 6-well plate at 3×10^5 cells before 24 h of transfection and cells were then transfected with 2000 ng of HMGB1 shRNA plasmid and shScrambled negative control plasmid. At 48 h and 72 h after transfection, the HEK293 cells were collected to evaluate methylation levels by COBRA assay.

TSA treatment

After plasmid transfection, cells were treated with 200ng/ml TSA (Sigma-Aldrich, St. Louis, MO, USA) for 6 hours.

จุฬาลงกรณ์มหาวิทยาลัย
Chulalongkorn University

RNA extraction, cDNA synthesis and real-time PCR

To observe mRNA expression, cells were harvested by trypsinization. The total RNA was isolated using Trizol reagent (Invitrogen) according to the manufacturer's instructions. Next, cDNA synthesis was performed by using 1000-3000 ng total RNA of each sample and RevertAid™ First Strand cDNA Synthesis Kit (Thermo Scientific). Real-time PCR was carried out using Power SYBR® Green PCR Master Mix (Applied Biosystems) with HMGB1 primers; HMGB1 forward (5'-ATATGGCAAAAGCG GACAAG-3') and HMGB1 reverse (5'-GCAACATCACCAATGGACAG-3'), SIRT1 primers; SIRT1 forward (5'GGTACCGAGATAACCTCCTG-3') and SIRT1 reverse (5'CATGTGAGGCTCT ATCCTCC-3'), and GAPDH (internal control) primers; GAPDH forward (5'-TGGAAGGACTCATGACCACAG-3') and GAPDH reverse (5'-TTCAGCTCAGGGATGAC CTT-3'). The amplification was performed in a 7500 Fast Real-Time PCR system (Applied Biosystems). The relative expression of genes was calculated with the 2-[$^{\Delta\Delta}$CT] method.

Alu siRNA transfection

siRNA of Alu transfection was be performed to increase methylation levels at Alu element. The sequences of siRNA-Alu are sense; 5'-CUUUGGGAGGCCGAGGCGGG CGGAUCA -3', antisense; 5'-AUCCGCCCGCCUCGGCCUCCCAAAGUG-3'. The day before transfection, Cells were seed at 50,000 cells per well of a 24-well plate in 500 ul of DMEM with 10% FBS. The transfection was performed by using Lipofectamine® 3000 Reagent following the manufacturer's protocol. A final concentration of Alu siRNA at 150 nM was used. Then, cells were incubated for 48 hours at 37 ˚C in a CO_2 incubator.

จุฬาลงกรณ์มหาวิทยาลัย
Chulalongkorn University

DNA Preparation and Sodium Bisulfite Treatment

Cells were collected by trypsinization, and extracted DNA with 10% sodium dodecyl sulfate (Sigma-Aldrich, MO, USA), lysis buffer II (0.75 M NaCl, 0.024 M ethylenediaminetetraacetic acid at pH 8) and 20 mg/ml proteinase K (USB, OH, USA) and incubated at 56°C overnights for cell digestion. DNA was extracted from digested cells

with phenol/chloroform and precipitated with absolute ethanol. Next, 750 ng of genomic DNA was subjected to sodium bisulfite treatment using the EZ DNA methylation-Gold™ kit (Zymo Research, CA, USA) according to the manufacturer's protocols. The eluted DNA was subsequently used for combined bisulfite restriction analysis (COBRA).

COBRA-Alu and COBRA-Alu-EDSB

COBRA-Alu was performed to measure the methylation of whole genome and COBRA-Alu-EDSB was used to measure the methylation near EDSB. Extracted HMW-DNA and genomic DNA was treated with sodium bisulfite using EZ DNA methylation-GoldTM kit (Zymo research) according to the manufacturer's protocol. For COBRA-Alu, the bisulfite-treated DNA was used to 35 cycles of PCR with primers, Alu-Forward; 5'-GGYGYGGTGGTTTAYGTTTGTAA-3' and Alu-Reverse; 5'-CTAACTTTTTATATTTTTAATA AAAACRAAATTTCACCA-3'. For COBRA-Alu-EDSB, the bisulfite treated HMW-DNA was set to 30 cycles of PCR for the first round with primers, B-linker LMPCR; 5'-GTTTGGAAGTTTATTTTGTGGAT-3' and Alu-Reverse; 5'-CTAACTTTTTATATTTTTAATAA AAACRAAATTTCACCA-3'. The PCR amplicons were then diluted for 1:10 and performed PCR to 40 cycles for the second round with primers, AluForward; 5'-GGYGYGGTGGTTTAYGTTTGTAA-3' and Alu-Reverse; 5'-CTAACTTTTTATATTTTTAAT AAAAACRAAATTTCACCA-3'. The 133 bp PCR amplicons were digested with two units of TaqI at 65 ˚C overnight. The gel was stain with SYBR green and intensity of DNA fragments were measured using Image Quant software (Molecular Dynamics, GE Healthcare, UK) as previously described (17).

จุฬาลงกรณ์มหาวิทยาลัย
Chulalongkorn University

HMWDNA preparation

Plugs were incubated at 16°C for 90 mins and washed with Tris-EDTA buffer for 20 mins 4 times. Ligation-mediated PCR (LM-PCR) linkers (5'-AGGTAACGAGTCAGACCACCGA TCGCTC-GGAAGCTTACCT-CGTGGACGT-3' and 5'-ACGTCCACGAG-3') were prepared and ligated to the polished DNA in plugs using T4 DNA ligase (New England Biolabs), and plugs were incubated at room temperature for

two nights. Then, HMWDNA was extracted from plugs using a TIANgel Midi Purification kit (Tiangen Biotech, Beijing, China).

DNA immunoprecipitation (DIP) of 8-OHdG

HMW DNA (1-1.5 μg) was sonicated for 7 mins with a Bioruptor (30 sec on 30 sec off at maximum power) to obtain 300-1,000 bp DNA fragments. The sonicated DNA was denatured at 95°C for 10 min and chilled immediately on ice. One-third of fragmented DNA was used as the input and two-third of DNA was incubated with 3-5 μg of antibodies overnight at 4 °C, including antibodies specific to DNA/RNA Damage antibody (8-OHdG) (abcam), Mouse IgG (abcam), and then incubated for 2 hours at at 4 °C with protein G Sepharose (GE Healthcare Life Sciences, Buckinghamshire, UK). After washing with phosphate-buffered saline, DNA was extracted from Sepharose beads by incubated with DIP digestion buffer and Proteinase K overnight at 50 °C. The DNA was extracted by phenol-chloroform method and resuspended in sterilized dH2O.

IRS-EDSB-LMPCR (DNA-GAP measurement)

IRS-EDSB-LMPCR or DNA-GAP PCR was prepared as previously reported (19). To determine EDSBs in cells, HMWDNA was carried out for DNA-GAP PCR by using a QuanStudio™ 6 Flex Real-Time PCR system (Thermo Fisher Scientific, MA, USA). The PCR components comprised 1x TaqMan™ Universal PCR Master Mix (Applied Biosystems, CA, USA), 0.5 U of HotStarTaq DNA polymerase (Qiagen, Hilden, Germany), 0.3 μM of probe homologous to 3'-linker sequence (6-fam) ACGTCCACGAGGTAAGCTTCCGAGCGA (tamra) (phosphate), 0.5 μM of human IRS primer (LINE-1) (5'-CTCCCAGCGTGAGCGAC-3') for human subjects or (Alu) (5'-ACTGCACTCCAGCCTGGGC-3'). Control DNA digested by EcoRV and AluI (Thermo Fisher Scientific, MA, USA) and ligated with linkers was used to generate a standard curve. The PCR cycle was set as follows: 1 cycle of 50°C for 2 mins followed by 95°C for

10 mins and 60 cycles of 95°C for 15 secs along with 60°C for 2 mins. The amount of DNA-GAP PCR in each test was compared to the digested ligated control DNA and reported as the percentage of DNA-GAP PCR amplicons of control DNA.

Cell viability assay

Cell viability was determined by 3-(4,5-dimethylthiazol-2-yl)-2,5-diphenyltetrazolium bromide (MTT) assays. After siAlu transfection for 48 h. The cells were collected and plated at 5,000 cells/well in 96-well plates. The following day, MTT was added to each well (Sigma-Aldrich) and incubated for 4 h. Subsequently 100 µl dimethyl sulphoxide (DMSO) was added to dissolve the formazan crystals. Absorbance was assessed with a Varioskan™ LUX multimode microplate reader (Thermo Scientific, MA, USA) at a wavelength of 570 nm.

Western Blot analysis

Cells were lysed in radio immunoprecipitation assay buffer (Sigma Chemical, St. Louis, MO USA) added protease inhibitors mixture (Pierce Biotechnology, Rockford, IL, USA). The protein concentration was quantified by BCA Protein Assay Kit (Thermo Scientific) according to the manufacturer's instructions. Thirty micrograms of whole cell lysate was separated using 12% sodium dodecyl sulfate (SDS) polyacrylamide gel electrophoresis and transferred to a nitrocellulose membrane. The signals were detected by Immobilon Western Chemiluminescent HRP Substrate (Merck, DA, Germany) and visualized by Azure c300 imaging systems (Azure biosystems, CA, USA). Antibodies used were as follows: 1:1000 HMGB1 (ab18256) (Abcam), 1:1000 SIRT1 (ab110304) (Abcam), 1:1000 Phospho-Histone H2A.X (Ser139) (9718s) (Cell signaling), 1:2000 goat anti-rabbit IgG-HRP (7074s) (Cell signaling), 1:2000 goat anti-mouse IgG-HRP (7076s) (Cell signaling),and anti-beta actin antibody [AC-15] (HRP) (ab49900) (Abcam, Cambridge, UK).

Nuclear extract

Transfected cells were collected and centrifuged for 10 mins at 3,000 rpm. Then, cells were performed nuclear isolation by using hypotonic buffer solution (20 mM Tris-HCl, pH 7.4, 10 mM NaCl, 3 mM MgCl2) and 10% NP40. The isolated nuclear pellet was resuspended in 50 µl PBS and 5 µl of nuclei fraction was smeared in 96-well plates and dried at room temperature for 30 min. Then, cells were fixed in 3.7% formaldehyde and permeabilized with 0.2% Triton X-100.

Colocalization assay

We performed DNA damage in situ ligation detected by proximity ligation assay (DI-PLA) to investigate colocalization between interested protein and Youth-DNA GAPs, and performed proximity ligation assay (PLA) to investigate protein-protein interaction. DI-PLA and PLA were performed following the manufacturer's protocol (Duolink® PLA detection reagent orange, DUO92007, Sigma-Aldrich, MO, USA). Briefly, the samples were permeabilized with 0.2% Triton X solution for 10 mins at room temperature. The samples were washed twice with PBS. One drop of Duolink® Blocking Solution was added and the sample was incubated for 60 min at 37°C. The nuclei were washed five times with PBS. Then, 100 µl of the blunting solution (1 mM dNTPs, 10 µl NEB buffer 2.1 (New England Biolabs, MA, USA), and 1 µl T4 DNA polymerase (5 U/µl, Thermo Fisher Scientific, MA, USA) was applied to the samples and the sample was incubated for 60 min at 16°C. The DI-PLA linker with biotin tagged was prepared in 50 µl of ligation solution (5 µl T4 ligase buffer 10x, 1.5 µl T4 DNA ligase (5 U/µls, Thermo Fisher Scientific, MA, USA), 0.5 µM DI-PLA linker, 0.2 mg/ml BSA. We added 50 µl of ligation solution to the samples and incubated them overnight at 37°C. Antibodies were diluted as indicate ratio with reaction buffer (1% FBS and 0.5% Tween 20 in PBS) and incubated for 3 hours at 37°C. Antibodies used in this experiment were shown in Table.1. Next, we incubated the samples with Duolink® PLA plus and minus probe diluted 1:50 with Duolink® antibody diluent for 2 hours at 37°C. The ligation reaction (1 µl Duolink® ligase, 8 µl Duolink®

ligation buffer, 32 µl dH2O) was prepared and added to the samples (60 min, 37°C). The amplification solution (0.5 µl Duolink® polymerase, 8 µl Duolink® polymerase buffer, 32 µl dH2O) was applied and incubated for 2 hours at 37°C. The samples were washed five times at room temperature. Finally, DAPI or Hoechst nuclear stain (1 µg/µl) was added and incubated for 10 min at room temperature. The positive fluorescent spots from the nucleus were visualized with a confocal microscope (20x and 40x). Positive fluorescent signal was evaluated as red spots in the nucleus of transfected cells. The positive cells with different numbers of positive signals from 1 to ≥ 9 spots were counted and classified in spot distribution. We calculated the percentage of positive cells by the number of positive nuclei divided by the total number of nuclei. All nuclei with positive spots were counted, and the fluorescence intensity was observed by CellSens® imaging software (Olympus® Co., Ltd., USA). The experiment was performed in triplicates.

Statistical analyses

Data were presented as the mean ± standard error mean (SEM). Statistical analyses were performed using PRISM Software 8.0 (GraphPad Software, CA, USA). Student's t test was performed to compare between two groups. For all analyses a two-sided p-value of < 0.05 was considered statistically significant.

Table 1. DI-PLA and PLA antibodies used in this study

Antibody	Dilution	Company
Anti-DDDDK tag (FLAG) mouse monoclonal antibody	1:1,000	Abcam, ab125243
Anti-DDDDK tag (FLAG) rabbit polyclonal antibody	1:1,000	Abcam, ab1162
Anti-SIRT1 mouse monoclonal antibody	1:1,000	Abcam, ab110304
Anti-biotin rabbit polyclonal antibody	1:1,000	Abcam, ab53494
Anti-γH2AX rabbit monoclonal antibody	1:1,000	Cell Signalling, 9817s
Anti-HA-tag mouse monoclonal antibody	1:250	Cell Signalling, 2367
Anti-HMGB1 rabbit polyclonal antibody	1:250	Abcam, ab18256
Goat anti-mouse-Cy3	1:1,000	Abcam, ab97035

จุฬาลงกรณ์มหาวิทยาลัย
CHULALONGKORN UNIVERSITY

CHAPTER IV
RESULTS

I Generation of stable knockdown HEK293

1. Virus transduction of HEK293 cells

Recombinant lentivirus packaging and production was done in 293T cells and the viral particle were then transduced into HEK293 target cell at the MOI of 5. HEK293 cells obtained virus constructs and were expressing GFP marker (Figure 7). The result from fluorescence microscopy was observed 48 h after infection.

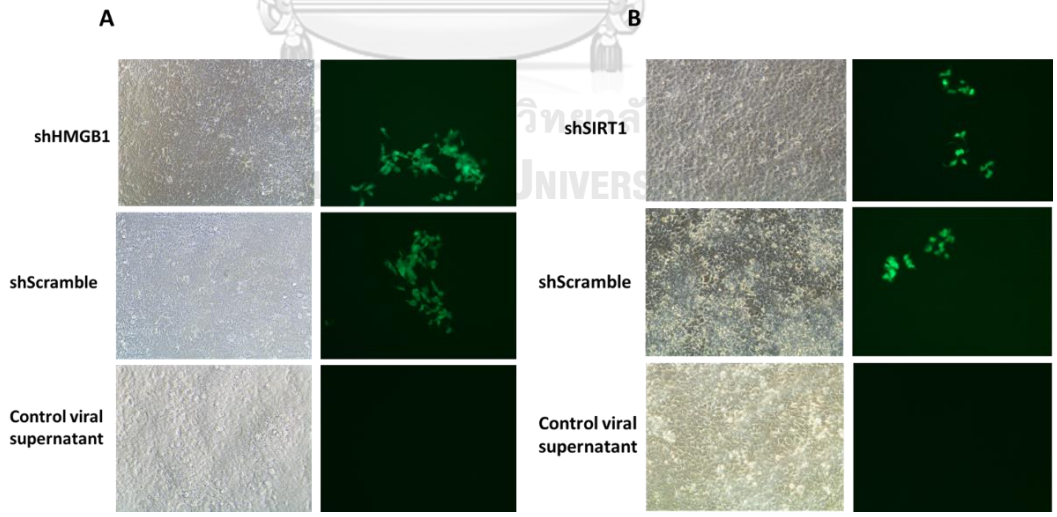

Figure 7. HEK293 cells express GFP after transduction with viral particle containing shRNA. Representative images of the HEK293 cell lines with expression GFP and the negative control viral particle in (A) HMGB1 knockdown cells (shHMGB1 and

shScramble) and (B) SIRT1 knockdown cells (shSIRT1 and shScramble). Cells were visualized under fluorescence microscope at 20X magnification.

2. HMGB1 and SIRT1 knockdown cells after puromycin selection

After 48-72 h after transduction, HEK293 cells transduced by HMGB1-shRNA or SIRT1-shRNA encoding lentivirus were treated with puromycin antibiotic at the final concentration of 1 ug/ml. Results showed that after 24 h of puromycin treatment at 1 ug/ml, cells without GFP expression died. Next, alive cells were then continued culture in medium containing puromycin for 4-6 weeks to get stable cell lines (Figure 8).

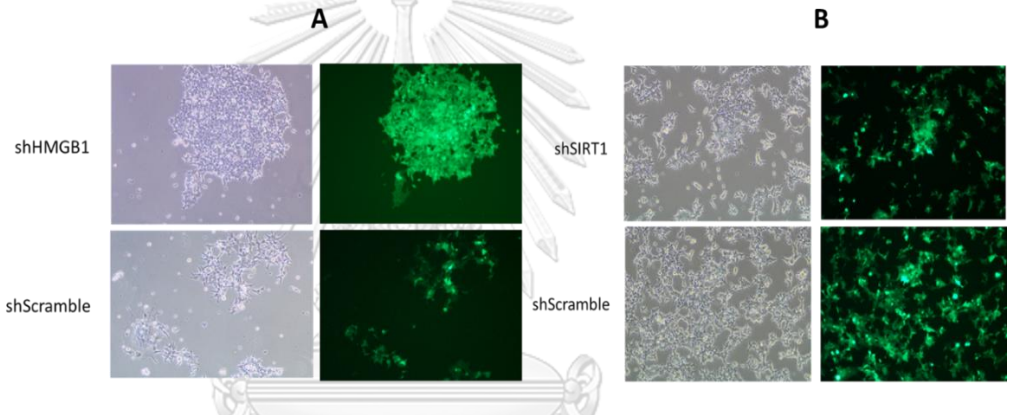

Figure 8. Lentivirus-mediated HMGB1- and SIRT1-shRNA knockdown of HEK293. Representative of Immunofluorescent images expressing GFP in (A) HMGB1 knockdown (shHMGB1) and control shRNA (shScramble) cells, and (B) SIRT1 knockdown (shSIRT1) and control shRNA (shScramble) cells. Cells were visualized under fluorescence microscope at 20X magnification.

CHULALONGKORN UNIVERSITY

3. Evaluation of stable HMGB1 knockdown HEK293 cells

To investigate the effect of HMGB1 shRNA on HMGB1 gene expression in HEK293 cells, real-time PCR assay performed and the expression of HMGB1 mRNA was compared between HMGB1-shRNA containing and Scramble-shRNA containing cells.

The data indicated that mRNA expression level of HMGB1 in shHMGB1 transduced cells was significantly reduced when compare to shScramble control cells. (Figure 9A). Moreover, western blot analysis also show lower protein expression level in shHMGB1 than those shScramble and HEK293 control cell (Figure 9B). Therefore, shRNA by RNAi is effectively inhibit HMGB1 expression.

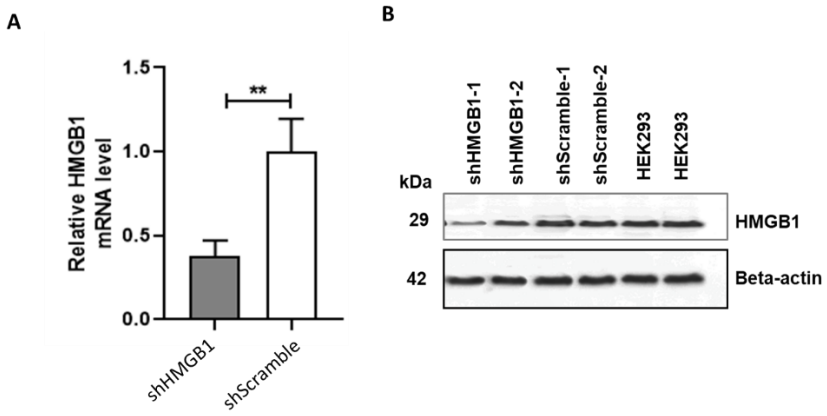

Figure 9. Real-time RT-PCR and western blot analysis confirmed the expression of HMGB1 stable knockdown cells. (A) mRNA expression by real-time PCR in shHMGB1 cells and shScramble cells. The relative mRNA level is presented as $2^{-\Delta\Delta}$CT. (B) Protein expression determined by western blot analysis in shHMGB1, shScramble and Negative HEK293 control cells. β-actin was used as internal control.

จุฬาลงกรณ์มหาวิทยาลัย
CHULALONGKORN UNIVERSITY

4. Evaluation of stable SIRT1 knockdown HEK293 cells

Real-time RT-PCR and western blot results confirmed the down-regulation of SIRT1 expression. shSIRT1 plasmids significantly suppressed the expression of SIRT1 mRNA, compared with the shScramble cells (Figure 10A). At the protein level, SIRT1 expression was weakened in shSIRT1 cells compared to shScramble cell and control HEK93 cells (Figure 10B). Thus, RNAi by shRNA effectively suppressed SIRT1 expression.

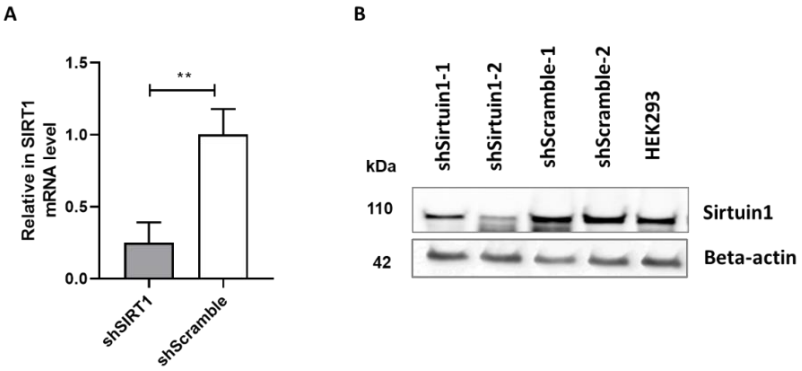

Figure 10. Real-time RT-PCR and western blot analysis confirmed the expression of SIRT1 stable knockdown cells. (A) mRNA expression of shSIRT1 cells and shScramble cells anylyzed by quantitative RT-PCR. SIRT1 knockdown (shSIRT1) normalized to controls (shScramble). The relative mRNA level is presented as $2^{-\Delta\Delta}$CT. (B) Immunoblot of SIRT1 expression in shSIRT1 cells (lane 1,2), shScramble cells (lane 3,4) and HEK293 cells (lane 5,6). β-actin was used as the control loading.

II HMGB1 producing RIND-EDSBs preventing genomic instability

1. Box-A of HMGB1 is a producer of Youth-DNA-GAPs

จุฬาลงกรณ์มหาวิทยาลัย
CHULALONGKORN UNIVERSITY

1.1. The number of Youth-DNA-GAPs was lower when HMGB1 was knockdown in human cells

To quantify the number of Youth-DNA-GAPs in cells lacking HMGB1, we measured the number of DNA-GAPs in HMGB1 knockdown cells by Alu-EDSB-LMPCR method. Using repetitive sequences that randomly scatter throughout the human genome, genome-wide EDSBs in proximity to Alu repeat were detected. As expect, the level of Youth-DNA-GAPs was significantly decreased in shHMGB1 cells compared to the shScramble control cells (Figure 11). This data indicates that Youth-DNA-GAPs are maintained or produced by HMGB1. Of note, there are two types of EDSBs in eukaryotic

genome; Youth-DNA-GAPs (physiologic RIND-EDSBs) and pathologic EDSBs, but under normal condition, the majority EDSBs is Youth-DNA-GAPs.

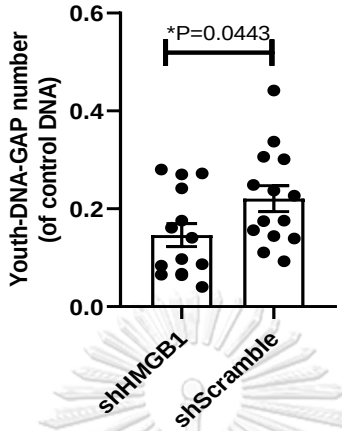

Figure 11. The levels of Youth-DNA-GAPs in HMGB1 knockdown. The levels Youth-DNA-GAPs in shHMGB1 cells and shScramble cells. The data are indicated as the mean±SEM. Statistical analysis using unpaired t-test. *p<0.05.

1.2. The number of Youth-DNA-GAPs was increased in HMGB1 and Box-A of HMGB1 overexpressed cells

จุฬาลงกรณ์มหาวิทยาลัย
Chulalongkorn University

To prove whether HMGB1 is a producer of Youth-DNA-GAPs, we employed DNA damage in situ ligation followed by proximity ligation assay (DI-PLA) to investigate whether which domain of HMGB1 produces the Youth-DNA-GAPs. DI-PLA assay can be used to detect physical DSBs in proximity of a target protein. The DNA ends of DSBs were ligated to a double-strand hairpin-shaped biotinylated DNA oligonucleotide, which permanently ligated all DSBs in the cells. Then, proximity ligation assay (PLA) was performed using antibody specific to biotin and antibody against the target protein which is nearness to the break. In this experiment, we transfected control plasmid (PC), HMGB1 plasmid and plasmid containing each domains of HMGB1 including, Box-A, Box-B, and Box BC. Moreover, we also transfected three Box-A mutant plasmids; p.Phe38Tyr (p.F38Y),

p.Phe38Trp (p.F38W) or p. Phe38Gly (p.F38G). After 24 h transfection, the expression was observed (Figure 12A). The number of positive cells were calculated by counting PLA spot (red) in the nucleus (Figure 12B). The results showed that the number of positive cells (%) was significantly increased in Box-A and HMGB1 transfected cells (Figure 12C). These findings reveal the role of Box-A in producing Youth-DNA-GAPs.

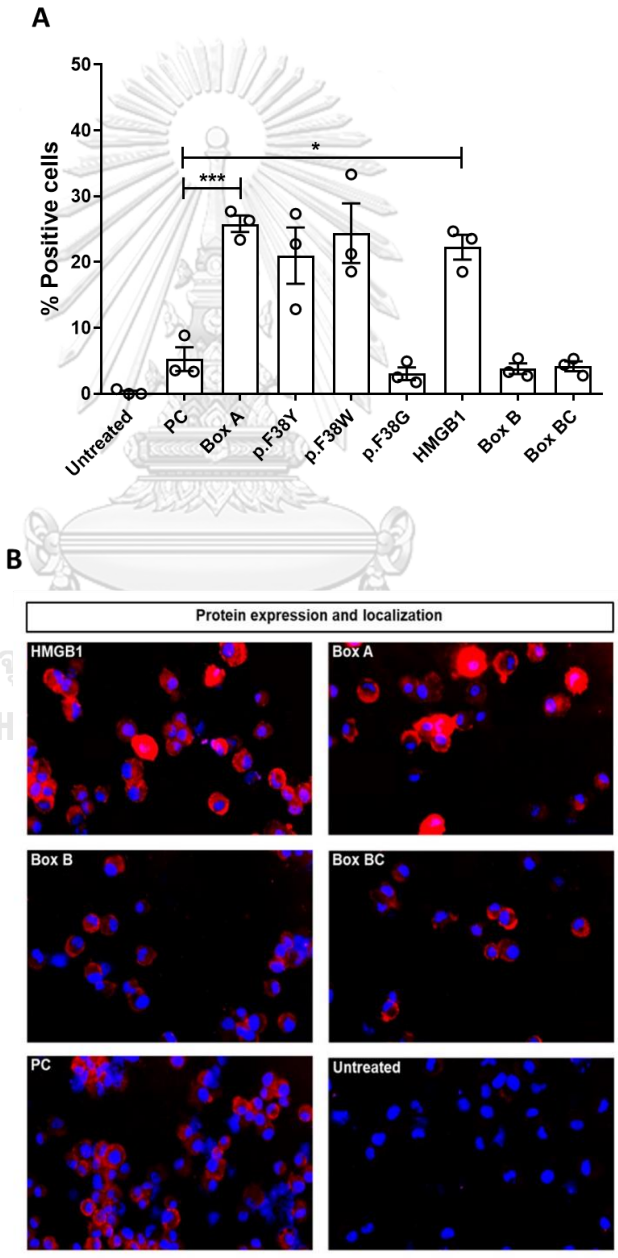

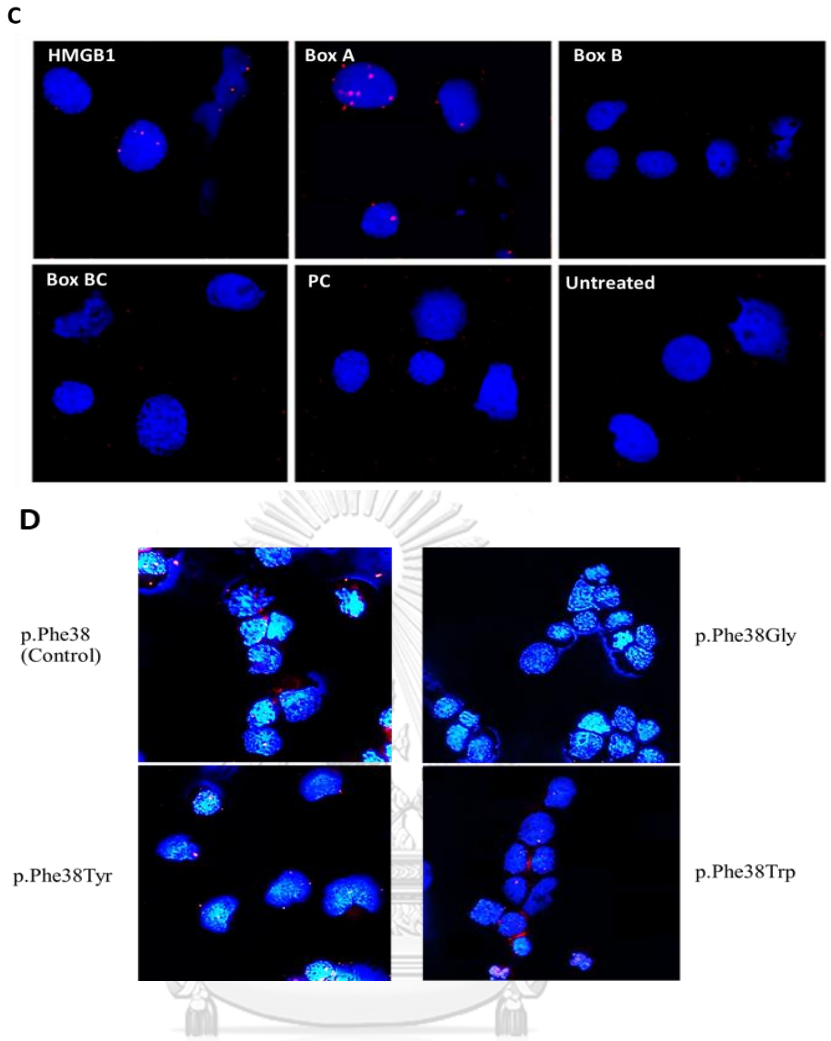

Figure 12. Co-localization of Box A and Youth-DNA-GAP by DI-PLA assay. (A) Bar graph representing the percentage of the number of positive (DI-PLA) in all transfected cells. (B) Immunofluorescence image of protein expression and localization using anti-DDDDK tag (FLAG) after transfection for 24 h. (C) Representative immunofluorescence of DI-PLA signal (red) signal using anti-FLAG and anti-biotin antibodies in HMGB1, Box-A, Box-B, Box-BC, PC, and untransfected cells and (D) in intact Box-A (p.Phe38), p.Phe38Tyr p.Phe38Gly, and p.Phe38Trp. Colocalization signal are shown in red and nuclei are shown in blue.

2. Youth-DNA-GAPs form complex with SIRT1

Previous study reported that the levels of Youth DNA-GAPs were decreased in yeast mutant SIR2 (SIRT1 in human) (19). Moreover, Youth-DNA-GAPs are localized in heterochromatin (20). The function of histone deacetylation is to protect Youth-DNA-GAPs from DSB response, **γ**-H2AX which is an early DSB response (18). Here, we evaluated the effect under histone deacetylase inhibition condition by chemical and molecular using Trichostatin (TSA) treatment (histone deacetylase inhibitor) and SIRT1 knockdown cells, respectively. We performed Proximity ligation assay (PLA) which can detect proteins that close proximity and quantified the number of PLA signal which represents the colocalization between Box-A (Youth DNA-GAP producer) and **γ**H2AX.

2.1 Co-localization of Box-A and γH2AX after TSA treatment

We tested whether Youth DNA-GAPs would be detected by DSB response, **γ**H2AX when the chromatin became acetylated. So, we transfected cells with Box-A plasmid and then treated the cells with TSA at 200 ng/ml. Next, PLA was utilized to test close proximity of our targets. Co-localization using anti FLAG –tagged and anti-**γ**H2AX is shown in Figure 13. Here, using PLA technique, we directly showed that Box-A colocalized extensively with **γ**H2AX after treated cells with TSA compared to no treatment, suggesting that Youth-DNA GAPs were retained by histone deacetylase before TSA treatment.

CHULALONGKORN UNIVERSITY

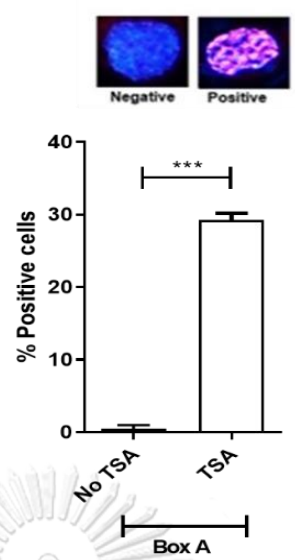

Figure 13. Detection of Box-A and γH2AX colocalization after TSA treatment by PLA assay. Comparison of percentage of positive cells in Box-A overexpressed cells with and without TSA treatment. The data are indicated as the mean±SEM from three independent experiments. ***p<0.001 t-test.

2.2 Colocalization of Box-A and γH2AX in SIRT1 knockdown cells

SIRT1 is a nicotinamide adenosine dinucleotide (NAD)-dependent deacetylase that removes acetyl groups and can deacetylate histone. We further investigate the effect of Box-A producing Youth-DNA GAPs in cells stably knocked down of SIRT1. shSIRT1 and shScramble cells were transfect with Box-A plasmids and examined colocalization by PLA. The result showed that the number of positive cells significant greater in shSIRT1 cells than shScramble cells (Figure 14).

จุฬาลงกรณ์มหาวิทยาลัย
Chulalongkorn University

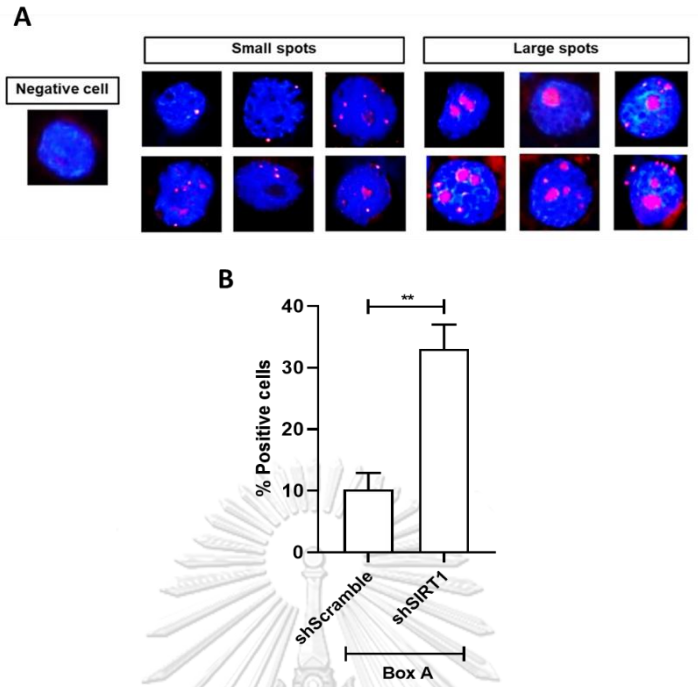

Figure 14. Colocalization staining of proteins from Box-A plasmid transfection and γH2AX. (A) PLA signal (red) of positive vs negative cells. (B) Percentage of positive cells with Box-A overexpression in shSIRT1 cells and shScramble cells. The data are represented as the mean±SEM from three independent experiments. **p<0.01.

จุฬาลงกรณ์มหาวิทยาลัย
Chulalongkorn University

2.3 Colocalization between Youth DNA-GAPs and endogenous SIRT1

Because we found that Youth DNA-GAPs were protected by SIRT1, we hypothesized that SIRT1 may form complex with Youth-DNA GAPs. We transfect Box-A and PC plasmid and then performed DI-PLA assay using anti-SIRT1 and anti-biotin that target DSBs. Result of DI-PLA indicates the close colocalization of Youth-DNA GAPs producing by Box-A and endogenous SIRT1 as shown in Figure 15.

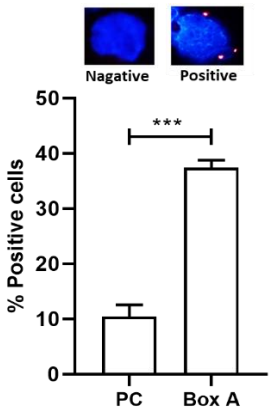

Figure 15. Colocalization of Youth DNA-GAPs and SIRT1 detected by DI-PLA. The number of positive DI-PLA cells in Box-A overexpressed cells was significantly increased compared to PC overexpressed cells. Data were independent biological samples (n=3). ***p < 0.001 t-test.

2.4 Box-A of HMGB1 interact with SIRT1

To test if Box-A of HMGB1 interacts with SIRT1, we performed PLA assay to detect protein-protein colocalization by using antibody against FLAG (DDDDK tag) and SIRT1. As shown in Figure 16, PLA assay indicates the interaction between Flag-tagged Box A and SIRT1.

จุฬาลงกรณ์มหาวิทยาลัย
CHULALONGKORN UNIVERSITY

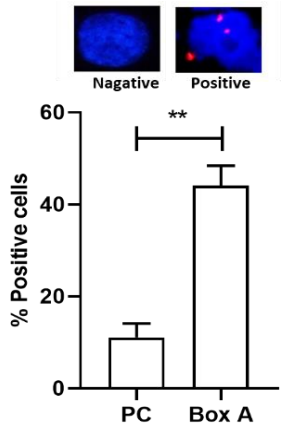

Figure 16. Box-A of HMGB1 interacts with SIRT1. Representative colocalization of transfected Flag-tagged Box A and SIRT1 (n = 3). Data are mean ± SEM **p <0.01.

3. The genome distribution of Youth DNA-GAP is far from DNA damage

It has been reported that the majority of EDSBs in yeasts with deletion of *HMGB1* homolog genes were pathologic EDSBs (19, 21). We hypothesized that if Youth DNA-GAPs have a role in preventing genomic instability by stabilizing the genome, the genome distribution of Youth DNA-GAPs should be located far from DNA damage. To determine the role of Youth DNA-GAPs in protecting DNA damages, overexpression of HMGB1 (Box-A, HMGB1, and PC control) and downregulation of HMGB1 (HMGB1 knockdown; shHMGB1 and shScramble control cell) were examined. Using IRS-EDSB LMPCR method can quantitatively measure both Youth-DNA-GAPs and pathologic EDSBs. However, under normal physiologic conditions, the major EDSBs detected in the cells are Youth-DNA-GAPs.

จุฬาลงกรณ์มหาวิทยาลัย
Chulalongkorn University

3.1. Youth DNA-GAPs prevent DNA damage; 8-OHdG

To determine the association between HMGB1 producing Youth DNA-GAPs and 8-OHdG, DNA immunoprecipitate (DIP) of 8-OHdG followed by IRS–EDSB LMPCR were performed. 8-OHdG, is a biochemical product of DNA damage which commonly used as a biomarker for oxidative damage to DNA. We measured the concentration of DNA-GAPs which were immunoprecipitated by 8-OHdG and compared with the whole genome. We

hypothesized that if the cells lack of HMGB1, a Youth-DNA-GAPs producer, the majority of EDSBs is pathologic EDSBs and these EDSBs lesions should be located near DNA damage. To calculate the percentage concentrations, the number of DNA gaps or EDSBs of the genome was normalized to 100%. As shown in Figure 17, DIP 8-OHdG results of shHMGB1 cells showed different data from others by which the concentrations of DNA GAPs was not different from the genomic DNA. Conversely, the concentrations 8-OHdG DIP DNA of the other groups (PC, Box-A, HMGB1, and shScramble) were lower than the genomic DNA. These results indicate the distribution pattern of 8-OHdG in which the DNA damage is prevented around Youth-DNA GAPs, suggesting a role of DNA GAPs in protecting DNA from DNA damage.

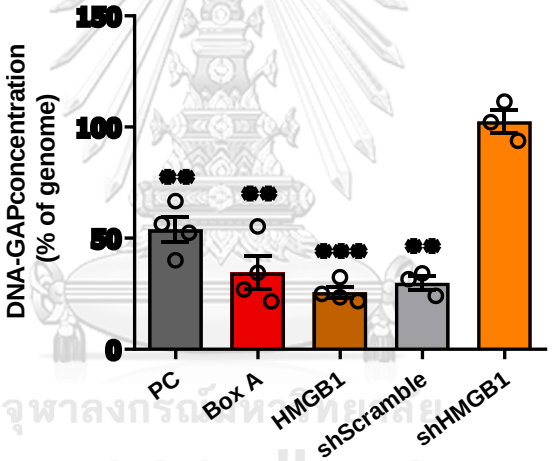

จุฬาลงกรณ์มหาวิทยาลัย
Chulalongkorn University

Figure 17. DNA-GAP PCR of DIP 8-OHdG PCR vs total genomic DNA.

The concentration of 8-OHdG-linked EDSBs quantified by DNA-GAP PCR products from DIP. Statistical analysis using paired t-test. Data are mean ± SEM **$p < 0.01$, and ***$p < 0.001$.

3. 2. Youth DNA-GAPs located distance from the DNA single-strand breaks

Next, we evaluated the distance from the DNA single-strand breaks (SSBs) to Youth-DNA-GAPs. Among different types of DNA damage. SSBs are the most common

DNA lesions that arise at a frequency of tens of thousands per cell per day (73). We hypothesized that the DNA protection effect spread out along the DNA strand from Youth-DNA-GAPs. Therefore, Youth-DNA-GAP should be reduced these DNA lesions. Mung bean nuclease enzyme was used to convert the SSBs to DSBs followed by IRS-EDSB LMPCR to quantify the level of DNA lesions from two locus types, IRS and EDSB. The IRS-SSB PCR represents SSBs which are genome-wide DNA damage, and EDSB-SSB PCR represents the distance of EDSBs from DNA damage. First, IRS-SSB PCR results confirmed the DNA protection role from DNA lesion of Box-A and HMGB1; in contrast to shHMGB1 by which the DNA lesion was higher than its control (shScramble) (Figure 18A). Second, EDSB-SSB PCR results in every groups, except shHMGB1 had a lower quantity than IRS-SSB-PCR. Interestingly, the amount of EDSB-SSB PCR products of shHMGB1 cells was extensively higher than others (Figure 18A). Taken together, these findings indicate that EDSBs generally located far from DNA damage than SSBs (IRS-SSB PCR). Moreover, the ratio of IRS/EDSB (proportion of IRS-SSB PCR and EDSB-SSB PCR product) demonstrated the distribution of EDSBs. IRS/EDSB ratios in most cells were a thousand-fold higher, but only shHMGB1 cells were just 4.7-fold higher (Fig. 18B).

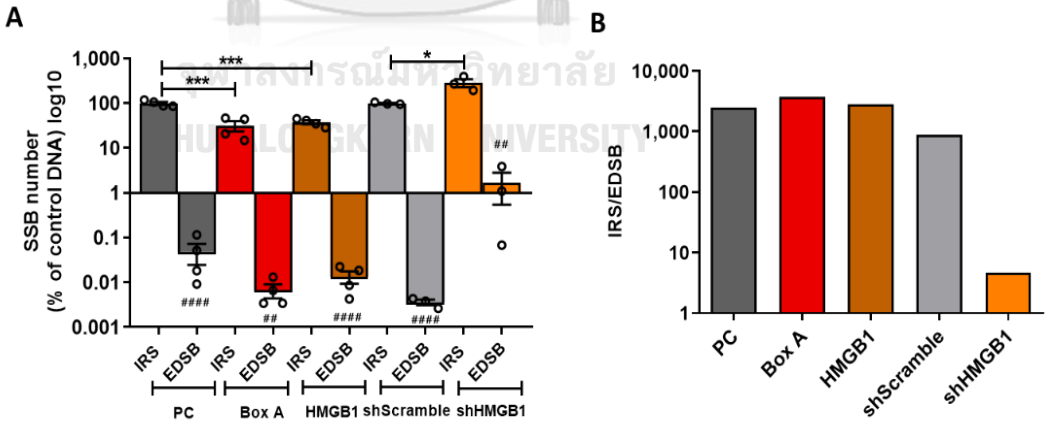

Figure 18. The comparison of IRS-SSB PCR and EDSB-SSB PCR. (A) Comparisons of two SSB PCRs product of cells overexpression with Box A, HMGB1 and PC control or shHMGB1 cells and shScramble cells. Data represent PCR levels of PC and

shScramble groups normalized to 100%. (B) The IRS/EDSB ratio in PC, Box A, HMGB1, shScramble, shHMGB1. Data are expressed as mean ± SEM. *p <0.05, ***p <0.001. ## p <0.01, ##### p<0.0001 when comparing IRS vs EDSB.

III. HMGB1 mediates DNA methylation to prevent genomic instability

1. Methylation levels (Alu) near Youth-DNA-GAPs was decreased in HMGB1 knockdown cells

It has been reported that Youth-DNA-GAPs are preferentially retained in methylated DNA (18, 20). Alu element repeat is one of the major transposons which distributes over million copies (approximately 11%) throughout the human genome; moreover, the decrease in its methylation has been associated with genomic instability. So, we decided to study this methylation status of this transposable element in our study. To test whether HMGB1 maintained methylated RIND-EDSB (Youth-DNA-GAPs), we therefore examined the methylation of Alu located near EDSBs in HEK293 cell depleted HMGB1. We modified COBRA-IRS LMPCR to measure Alu methylation levels at sites close to RIND-EDSBs (Youth-DNA-GAPs). We found that methylation of Alu located near EDSB was significant decreased in HMGB1 knockdown cells when compared to control cells (Figure 19).

ALUNGKORN UNIVERSITY

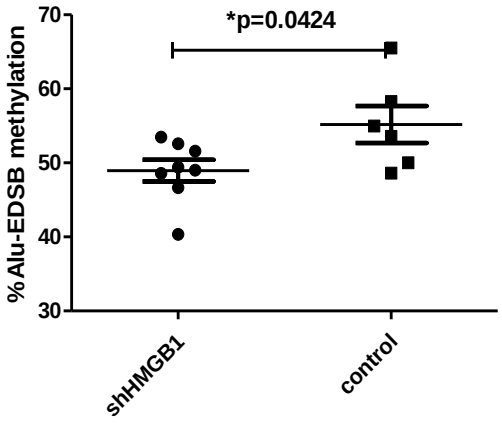

Figure 19. Levels of Alu methylation located near EDSBs in HMGB1 knocked down cells. Percentage of Alu-EDSB methylation detected by COBRA-IRS in shHMGB1 cells and control (scrambled shRNA) cells. Data from independent experiments presented as the mean±SEM. Statistical analysis using unpaired t-test. *p<0.05.

2. Reduction of genomic Alu methylation in HMGB1 downregulation

To determine whether HMGB1 also has an impact on IRS methylation, Alu element, we employed transient transfection using shRNA-mediated silencing of HMGB1. HEK293 cells were transfected with HMGB1-shRNA plasmid and control Scrambled-shRNA plasmid and measured the levels of Alu methylation. After transfection for 48 h and 72 h, the methylation levels of Alu were examined by COBRA assay. The protein levels in cells silent HMGB1 were confirmed by western blot analysis. After knocking down HMGB1 at 48 h and 72 h, we observed higher protein levels in Scramble shRNA transfected- and untransfected HEK293 cells (control) than shRNA against HMGB1 transfected cells (Figure 20A). The result showed that down-regulation of HMGB1 resulted in a significant decrease of Alu methylation levels, and this effect was time-dependent manner (Figure 20B). These data reveal a correlation between loss of HMGB1 and IRS hypomethylation by which silencing of HMGB1 caused lower Alu methylation levels.

จุฬาลงกรณ์มหาวิทยาลัย
Chulalongkorn University

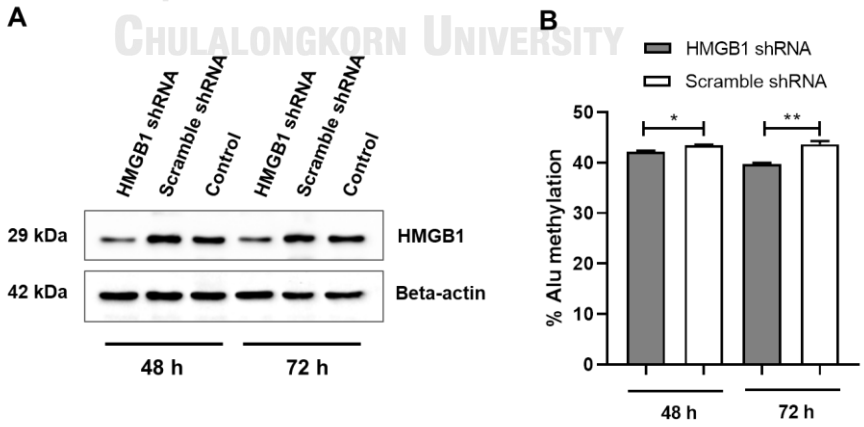

Figure 20. Downregulation of HMGB1 reduces genomic Alu methylation levels. (A) Confirmation of HMGB1 protein levels in the time course of plasmid transfection by

western analysis in HMGB1 shRNA, Scramble shRNA transfected- and untransfected HEK293 cells. Beta-actin was used as an internal control. (B) The percentage of Alu methylation in HEK293 cells transfected with HMGB1 shRNA plasmid and Scrambled shRNA plasmid at 48 h and 72 h. Statistical analysis was performed using student's t-test: *p<0.05, and **p<0.01.

3. Alu methylation increases in HMGB1 overexpression

We further asked whether HMGB1 itself can induces Alu methylation. We investigated Alu methylation levels at 48, 72, and 96 hours in HEK293 cells overexpression of HMGB1 and also Box-A of HMGB1. In HMGB1 overexpressed cells, the significant increase of Alu methylation levels were detected at 72 h and 96 h. Moreover, we observed a higher level of Alu methylation in Box- A overexpression than the plasmid control (PC) after transfection for 96 h (Figure 21). These findings confirm the connection between HMGB1 and Alu methylation, suggesting the role of HMGB1 in participating in IRS DNA methylation.

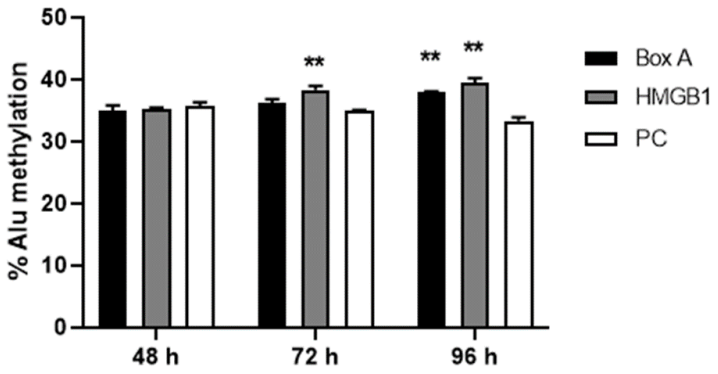

Figure 21. Overexpression of HMGB1 increases genomic Alu methylation levels. The percentage of Alu methylation in HEK293 cells overexpression with Box-A, HMGB1, and PC plasmid at 48, 72, and 96 h. Statistical analysis are shown as the mean±SEM. **p<0.01 t-test.

4. HMGB1 is required for IRS methylation by RdDM machinery

In plants and humans, an important role in silencing of transposable elements is regulated through DNA methylation using small interfering RNAs (siRNA) or RdDM. We asked whether IRS DNA methylation which is controlled by RdDM process, is related to HMGB1. To gain insight into the potential role of DNA methylation contributing of TEs silencing in human whether HMGB1 is implicated in this molecular event. We performed AGO4 and Alu siRNA transfection in cells lacking HMGB1 and investigate Alu methylation.

4.1. Alu methylation promoted by Alu siRNA is mediated by HMGB1

Previous study demonstrated that Alu element siRNA (siAlu) transfection increased methylation specifically at Alu (17). To determine whether HMGB1 is required to induce Alu methylation by Alu siRNA (siAlu). Alu methylation level was observed in cell knockdown of HMGB1 after siAlu transfection. The stable HMGB1 knockdown (shHMGB1), control Scrambled shRNA (shScramble) cells as well as HEK293 cells were transfected with siAlu and Alu methylation level were then evaluated by COBRA assay. As shown in Figure 22A-D, compared with lipofectamine control reagent (lipofect), a significant increase of Alu methylation levels was found in cell existing HMGB1, shScramble and HEK293. Conversely, we did not find any significant of Alu methylation level when HMGB1 was suppressed. This finding indicates that Alu methylation by Alu siRNA is HMGB1 dependent.

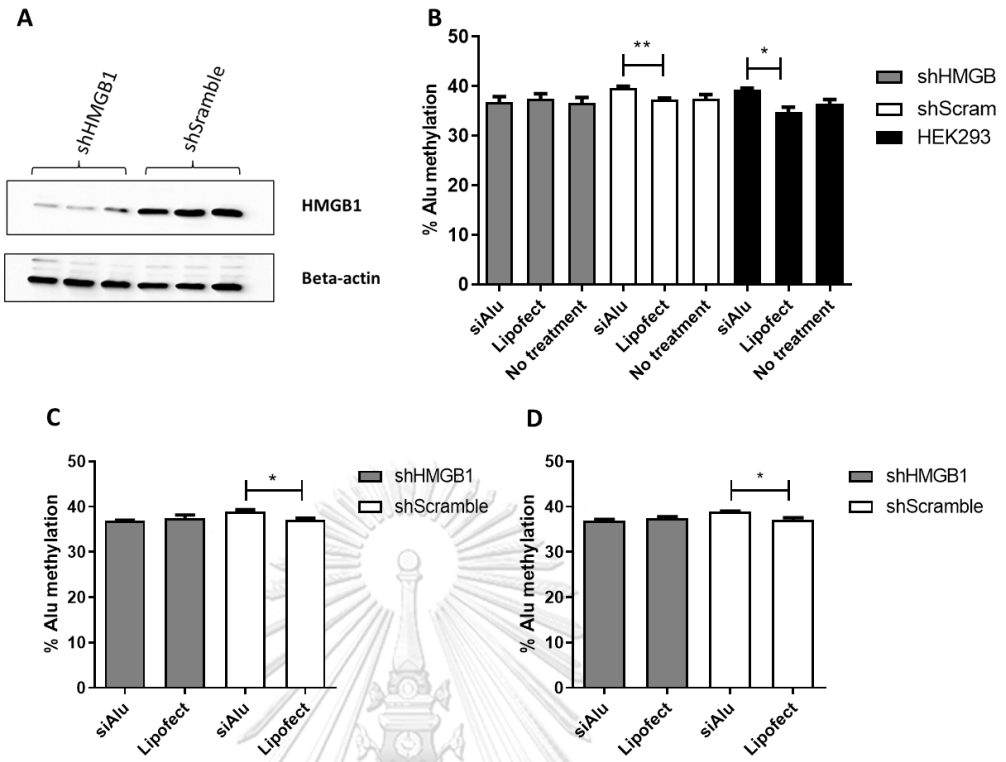

Figure 22. Alu methylation level upon Alu siRNA transfection in HMGB1 knockdown cells. (A) Confirmation of HMGB1 expression in stable HMGB1 knockdown cells. (B) The percentage of Alu methylation levels of shHMGB1 (gray), shScramble (white) and HEK293 cell lines (black) in siAlu (150 nM) transfection, Lipofectamine reagent (Lipofect) transfection, and HEK293 cells without transfection. (C-D) The percentage of Alu methylation of shHMGB1 (gray), shScramble (white) in siAlu transfection and Lipofect transfection (control). The data are indicated as the mean±SEM. *p<0.05., **p<0.01.

จุฬาลงกรณ์มหาวิทยาลัย
Chulalongkorn University

4.2 Overexpressed AGO4 did not affect Alu methylation in HMGB1 knockdown cell

AGO4 can promote methylation at IRS, such as Alu (16). To examine whether AGO4 inducing methylation is associated with HMGB1, we also tested Alu methylation level after AGO4 transfection in HMGB1 knockdown. We found that only AGO4 overexpressed HEK293 cells had significantly higher of Alu methylation than PC control overexpressed HEK293 cells. In contrast, shHMGB1 and shScramble cells did not showed any significant differences (Figure 23).

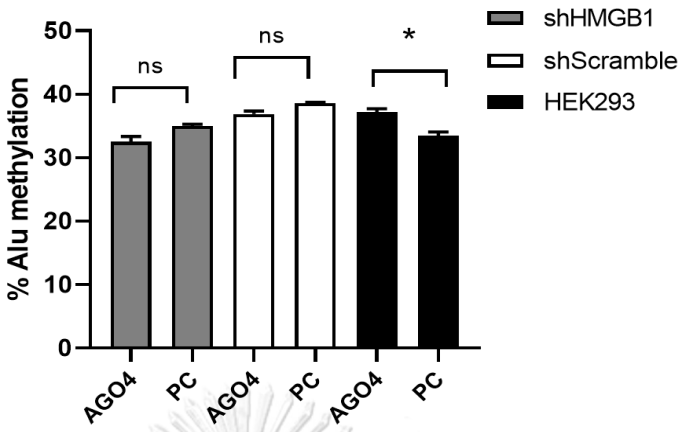

Figure 23. Alu methylation level upon AGO4 transfection in HMGB1 knockdown cells. The percentage of Alu methylation levels of shHMGB1 (gray), shScramble (white), and HEK293 (black). The Alu methylation level was significantly increased when AGO4 was upregulated in HEK293. The data are indicated as the mean±SEM. *p<0.05.

5. HMGB1 interacts with AGO4 protein

Since we explored the interplay between HMGB1 and RdDM mediating *de novo* methylation by Alu siRNA. We hypothesized that HMGB1 might collaborate with a protein that cans *de novo* methylate by siRNA. Furthermore, a recently report has been clarified that AGO4 not only act as a major protein in human RdDM but this machinery is also AGO4 dependent (16). Therefore, we further investigated the protein-protein interaction of HMGB1 and AGO4. HEK293 cells were overexpressed with HA-tagged AGO4 plasmid or pcDNA3.1 (PC) plasmid. Subsequently, proximity ligation assay (PLA) was employed to detect their close proximity of two proteins; ectopically expressed AGO4 and endogenously expressed HMGB1. The interaction of AGO4 and endogenous HMGB1 was observed in cell overexpression HA-tagged AGO4 and microscopically displayed the localization between AGO4 and endogenous HMGB1 in the nucleus, as shown in Figure

24. Therefore, these observations indicate that HMGB1 interact with AGO4 and participates in human RdDM.

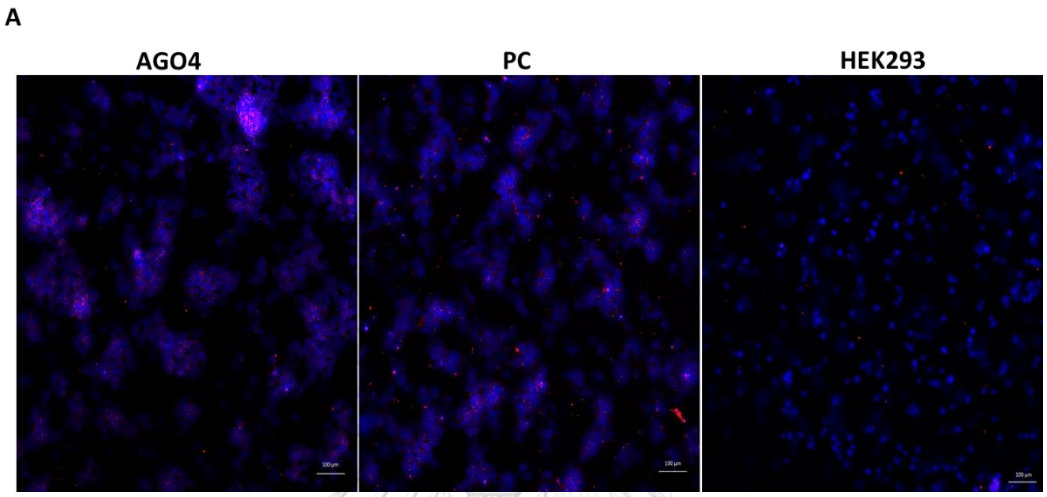

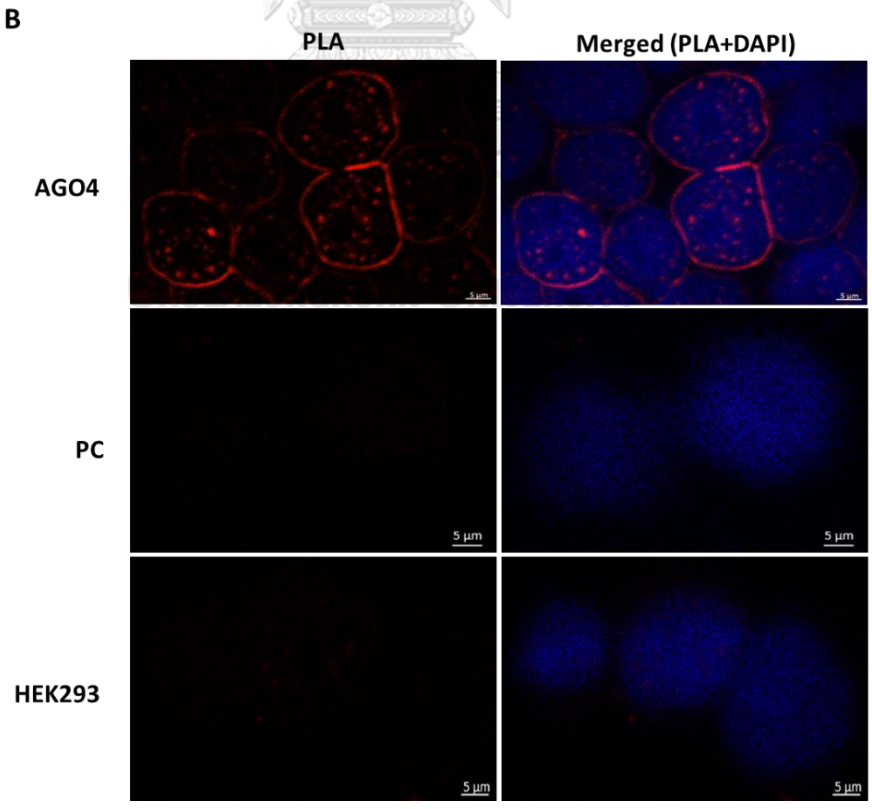

Figure 24. The interaction between AGO4 and HMGB1 protein by proximity ligation assay. In-situ PLA assay illustrates the colocalization between HA-tag AGO4 and HMGB1 (A) image at low magnification in AGO4- and PC-transfected cells as well as untransfected HEK293 cells. Scale bar = 100 μm (B) Immunofluorescence image at higher magnification. Scale bar = 5 μm. PLA signals were shown in red and nuclei were stained using DAPI (blue). PLA signal was visualized under Zeiss LSM800 confocal laser scanning microscope.

6. HMGB1 is required DNA methylation to prevent genomic instability

6.1 Cell viability under Alu siRNA transfection was not increased in stably knocking down HMGB1 cells

To evaluate the effect of Alu siRNA on cell viability when HMGB1 was stably inhibited, MTT assay was performed after 48 h of siAlu transfection. siAlu transfected cells were measured cell growth compared with their control (lipofectamine). It was showed that only siAlu transfection in scrambled cells (shScramble) had a significant effect on cell viability while siAlu transfected-HMGB1 knockdown cells (shHMGB1) inhibited cell proliferation (Figure 25), suggesting that even though Alu siRNA transfection, HMGB1 attenuates cell survival.

จุฬาลงกรณ์มหาวิทยาลัย
Chulalongkorn University

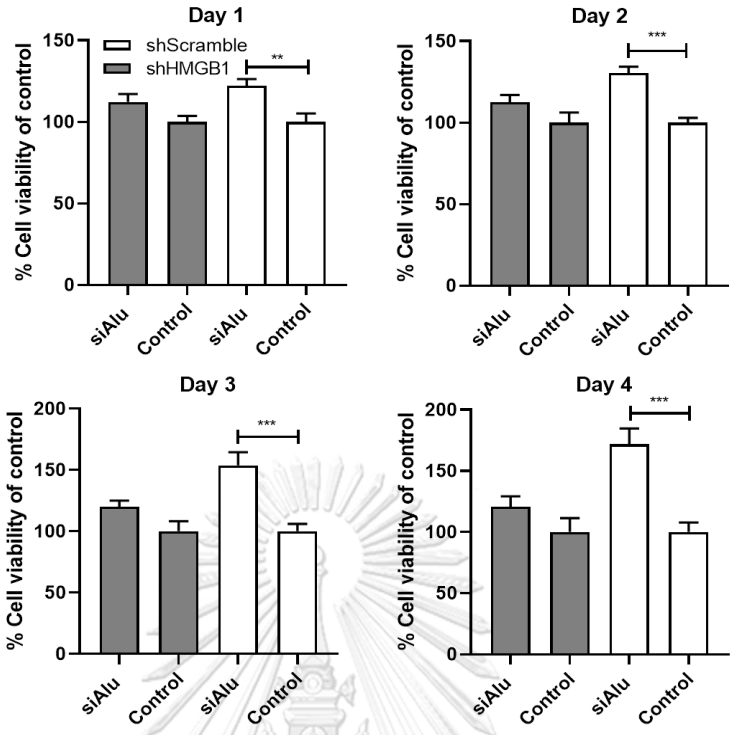

Figure 25. Cell viability of Alu siRNA transfection under stably knockdown of HMGB1. After 48h post-transfection, the transfected cells were seed into 96-well plates to assess cell viability by MTT assay over four days. Cell viability was significantly increased in shScramble cells after siAlu transfection. MTT results are expressed as mean ± SEM. **p<0.01 and **p<0.001 unpaired t-test.

จุฬาลงกรณ์มหาวิทยาลัย
CHULALONGKORN UNIVERSITY

6.2. γH2AX level was decreased in siAlu- and AGO4-transfected cells

AGO4 overexpression increased IRS methylation, including Alu element (16). Hypermethylation at IRS especially at Alu repeats maintains genome stability by reducing endogenous DNA damages (17). To shed light on this epigenetic role in protecting genomic instability, we investigated the protein levels of phosphorylated histone H2AX (γH2AX), a biomarker representing DNA damage and genomic instability after transfected HEK293 cells with siRNA (Alu siRNA) or AGO4-expressing plasmid which are key components in RdDM complex. The results from western blot analysis showed that cells transfected with Alu siRNA and AGO4 showed lower γH2AX levels than their control

counterpart, lipofectamine transfection reagent and PC, respectively as shown in Figure 26A and 26B.

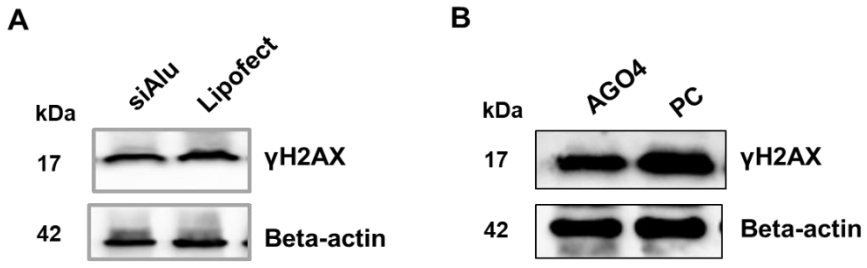

Figure 26. Detection of γH2AX by western blot analysis in (A) siAlu and lipofectamine transfection in HEK293 for 48 h and (B) AGO4 and PC transfected HEK293 cells at 72h.

6.3. γH2AX of siAlu- and AGO4- transfected cells was not decreased when HMGB1 was stably inhibited

We further determine the effect of HMGB1 on genomic instability prevention whether it is related to RdDM mediating IRS methylation. The transfections were applied to stable HMGB1 depleted cells (shHMGB1). In both siAlu- and AGO4 transfected shScramble cells, the expression of γH2AX at the protein levels analyzed by western blotting was significantly lower than those controls. In contrast, stable HMGB1 knockdown cells (shHMGB1) tend to show increased γH2AX levels (Figure 27). These findings demonstrate that lacking of HMGB1 restricts the role of Alu siRNA and AGO4 on genomic instability prevention.

จุฬาลงกรณ์มหาวิทยาลัย
Chulalongkorn University

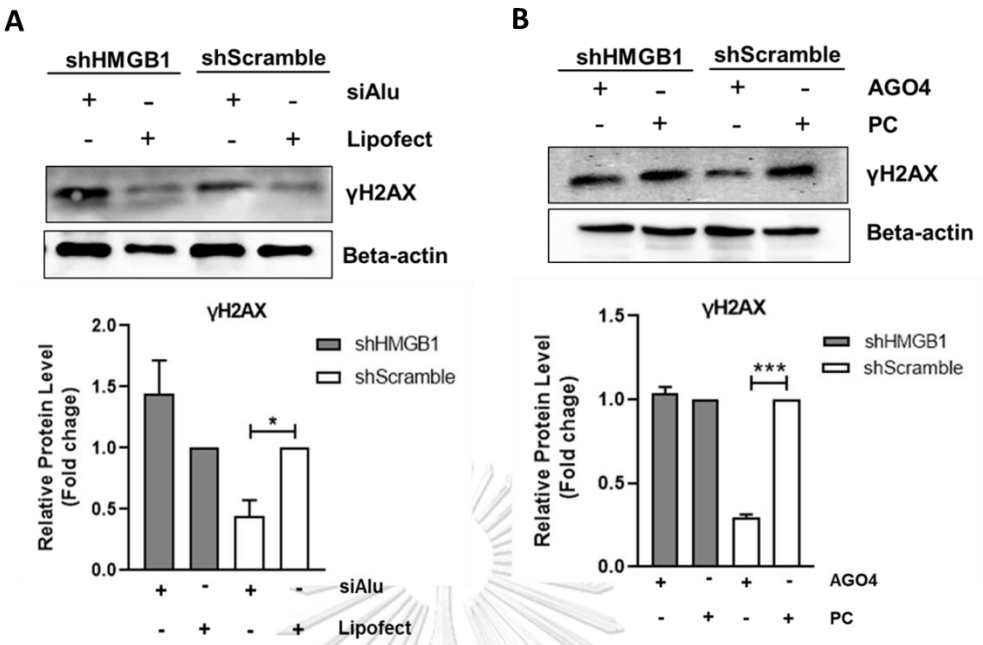

Figure 27. Immunoblot of γH2AX in siAlu- and AGO4-transfected cell upon HMGB1 knockdown. (A) Representative western blots (Top) and the bar graph showing statistical analysis (Bottom) of γH2AX expression. HMGB1 knockdown cells (shHMGB1) and control cells (shScramble) were transfected with Alu siRNA (siAlu) and Lipofectamine. (B) Immunoblot (Top) and the statistical results (Bottom) of γH2AX level. HMGB1 knockdown cells (shHMGB1) and control cells (shScramble) were transfected with AGO4 plasmid (AGO4) or empty plasmid (PC). The data are presented as the mean ± SEM. *p<0.05, ***p<0.001.

จุฬาลงกรณ์มหาวิทยาลัย
Chulalongkorn University

CHAPTER V
DISCUSSION

HMGB1 producing Youth-DNA-Gaps preventing genomic instability

In this current study, we demonstrated that HMGB1 is a pivotal protein that can play an essential role in mediating DNA methylation to prevent genomic instability. First, HMGB1 generates and maintains physiologic RIND-EDSBs or Youth-DNA-GAPs in methylated genome. Second, HMGB1 formed Youth-DNA-GAPs complex and SIRT1 protected Youth-DNA-GAPs from DNA damage response. Third, the genome distribution pattern of Youth-DNA-GAPs was far from DNA damages and Youth-DNA-GAPs stabilized genome in long distances. Finally, HMGB1 is required for DNA methylation through RdDM machinery to prevent genomic instability.

First, we addressed that Box-A of HMGB1 generates Youth-DNA-GAPs (physiologic RIND-EDSBs). We determined the levels of Youth-DNA-GAPs in two conditions; downregulation and overexpression of HMGB1. The lower number of Youth DNA-GAPs was detected in HMGB1 knockdown cells performed by IRS-EDSB LMPCR assay. In contrast, the results from DNA Damage In Situ Ligation Followed by Proximity Ligation assay (DI-PLA) showed a higher number of Youth DNA-GAPs in cell overexpression of HMGB1 and particularly in Box A. Using DI-PLA assay, we can detect close localized between physical DSBs and our target proteins (FLAG-tagged). This data suggests that Box A (Phe 38) domain of HMGB1 is a producer of Youth-DNA-GAPs. These results are consistent with our previous study that demonstrated the role of HMGB1 in maintaining Youth-DNA-GAPs (19).

Next, we further explored the formation of Youth-DNA-GAPs complex. Our previous study reported earlier that Youth-DNA GAPs are localized in heterochromatin (20). Moreover, the levels of Youth DNA-GAPs were decreased in yeast mutant SIR2

จุฬาลงกรณ์มหาวิทยาลัย
Chulalongkorn University

(SIRT1 in human) (19). We evaluated the effect under histone deacetylase inhibition condition by chemical and molecular by Trichostatin (TSA) treatment (histone deacetylase inhibitor) and SIRT1 downregulation, respectively. Using in situ proximity ligation assay (PLA), we identified that Box-A colocalized with γH2AX after TSA treatment and in SIRT1 knockdown cells, these observations indicate that Youth-DNA-GAPs were retained by histone deacetylase. Although Youth-DNA-GAPs are EDSBs, chromatin condenses to protect Youth-DNA-GAPs from the DSB response, γH2AX. Our results showed a crucial role of histone deacetylation in preventing Youth-DNA-GAPs from γH2AX (20). In addition, SIRT1 are colocalized with Youth-DNA-GAPs and Box-A of HMGB1. These data demonstrate the defensive role of Box A-induced DNA gaps from γH2AX via histone deacetylation of SIRT1. As a result, it can be concluded that SIRT1 play a role in Youth-DNA-GAP protection.

Here, we conducted two novel PCR methods that able to analyzed DNA damage that present around EDSBs; 8-OHdG and single strand breaks DNA (SSB). It has been proposed that DNA lesions occurred in human cells with approximately 70,000 lesions per day, and the majority of lesions (approximately 75%) are single-strand DNA (ssDNA) breaks, which are a result from oxidative damage during metabolism or base hydrolysis (73). Moreover, 8-OHdG is one of the most common lesions that arise from reactive oxygen which can result in mispairing with adenine resulting in G>T substitutions (74). Therefore, we selected these two DNA lesions to study the association and distribution pattern of Youth-DNA-GAPs in whole genome. First, we modified DNA immunoprecipitation (DIP) assay by selected DNA that immunoprecipitated with 8-OHdG antibodies followed by IRS-EDSB LMPCR to evaluate the distance from single strand breaks DNA (SSB) to Youth-DNA-GAPs. Second, IRS-SSB PCR combined with EDSB-SSB PCR were used to analyze the amount of SSBs and evaluated the distance between Youth-DNA-GAPs and SSBs, respectively. The quantity of EDSB-SSB PCR negatively correlates with the genomic distance between EDSB and SSB. The analysis in both PCR also confirms the distribution of Youth-DNA-GAPs that EDSBs, in general, were located more distant from DNA damages. The flexible DNA structure by Youth-DNA-GAPs produed by

จุฬาลงกรณ์มหาวิทยาลัย
CHULALONGKORN UNIVERSITY

HMGB1 may be an underlying mechanism that protect DNA from insults. Because when the DNA ends were fixed, its movement energy caused torsional force to destabilize DNA (75-77). Even though bending of the DNA disturbs the hydrogen bonds in DNA strands, HMGB1 can bend DNA and stabilize it against denaturation (78), leading to low numbers of DNA lesions in the genome.

HMGB1 mediates DNA methylation to prevent genomic instability

The analysis of Alu methylation in HMGB1 knockdown demonstrates that lacking of HMGB1 causing the reduction of not only methylation near Youth-DNA-GAPs but also genomic methylation. The methylation pre-exist at Youth-DNA-GAPs (hypermethylated RIND-EDSB) is higher than the cellular genome (18) while pathologic EDSBs normally have lower methylation (hypomethylation) than the rest genome. Additionally, several pieces of evidences have been proved that genomic instability as a result of genome-wide hypomethylation (3-5). Therefore, it can be referred that loss of HMGB1 reducing methylated RIND-EDSBs causes global hypomethylation which is a precursor of genomic instability. Here, we demonstrated the first evidences that loss of HMGB1 caused global hypomethylation (representing by Alu), and HMGB1 overexpression leads to hypermethylation at IRS, Alu repetitive sequence, indicating a role of HMGB1 in participating IRS methylation. It has been reported that loss of nuclear HMGB1 resulted in cell senescence (79). Global hypomethylation is an early molecular event leading cell senescence, including cancers (5-8). We postulate that releasing of nuclear HMGB1 may be an initiator and driver human carcinogenesis.

Since we identified the effect of HMGB1 on genome-wide methylation, we further investigate the association on DNA methylation level between HMGB1 and RdDM by which DNA methylation is induced by small non-coding RNA. This mechanism is essential for the genome in protecting global hypomethylation in repetitive sequences. First, we found the interaction between HMGB1 and AGO4 using proximity ligation assay. More insight mechanism are need for further studies whether which domain of HMGB1 is

responsible the binding. Second, Alu methylation induced by Alu siRNA is HMGB1 dependent. When HMGB1 was limited, siAlu could not promote Alu methylation while in cells presented HMGB1, significant increase of Alu methylation was observed (shScramble and untransfected HEK293 cells). This result is in accordance with the study of Patchsang et al. (17), Third, AGO4 transfection did not induce Alu methylation in HMGB1 knockdown cells. Of note, we did not find an increased level of Alu methylation in shScramble cells. This may be from the reasons; first, Scramble shRNA itself produces siRNA which may be able to bind some of Alu repetitive sequences and consequently methylated DNA (CpG), or AGO4 can localize to both IRS LINE-1 and Alu, but we detected only Alu methylation. So, we cannot observed the methylation changes at Alu. Nevertheless, a higher level of Alu methylation was investigated in AGO4 transfection compared to empty plasmid control in HEK293 cells. Our data is similar to previous results by which AGO4 preferentially bound to IRS and induced specifically at those loci (16).

Furthermore, we also study the effect of HMGB1 knockdown linking genomic instability after Alu siRNA and AGO4 transfection. Our results demonstrate that DNA methylation (RdDM) preventing genomic instability is depended on the function of HMGB1. To examine the effect on cell survival, MTT assay was performed after siAlu transfection. It was showed that cell viability was not increased in HMGB1 depleted cells. Next, we investigated the role of HMGB1 on genomic instability prevention. The expression of γH2AX was analyzed. γH2AX is a highly specific and sensitive molecular marker for monitoring DNA damage. γH2AX responses early after the induction of DNA double-strand breaks (80). Western blot analysis demonstrated that despite siAlu or AGO4 transfection, HMGB1 downregulation augmented γH2AX protein levels, suggesting that the role of HMGB1 on genomic instability protection is RdDM dependent. In HMGB1 knockdown, neither siAlu/ AGO4 increased Alu methylation nor reduce DNA damage. These observations provide a role of HMGB1 that it not only affects methylation but also prevent genomic instability.

จุฬาลงกรณ์มหาวิทยาลัย
Chulalongkorn University

In conclusion, this study uncovers the role of HMGB1 in mediating DNA methylation. DNA methylation plays a vital role to prevent genomic instability. HMGB1 mediates DNA methylation by producing methylated RIND-EDSBs or Youth-DNA-GAPs, and maintaining Youth-DNA-GAPs by form the complex with SIRT1. Loss of HMGB1 causes decreased in methylation levels, both Youth-DNA-GAPs and whole genome, and consequently induces genomic instability. Therefore, this mechanism provides us an understanding of how global hypomethylation promoting genomic instability. Our study propose two mechanisms of HMGB1 mediates DNA methylation preventing genomic instability. One is Youth-DNA-GAP production then recruits DNA methylation or another one is DNA methylation then Youth-DNA-GAP production (Figure 28A and 28B).

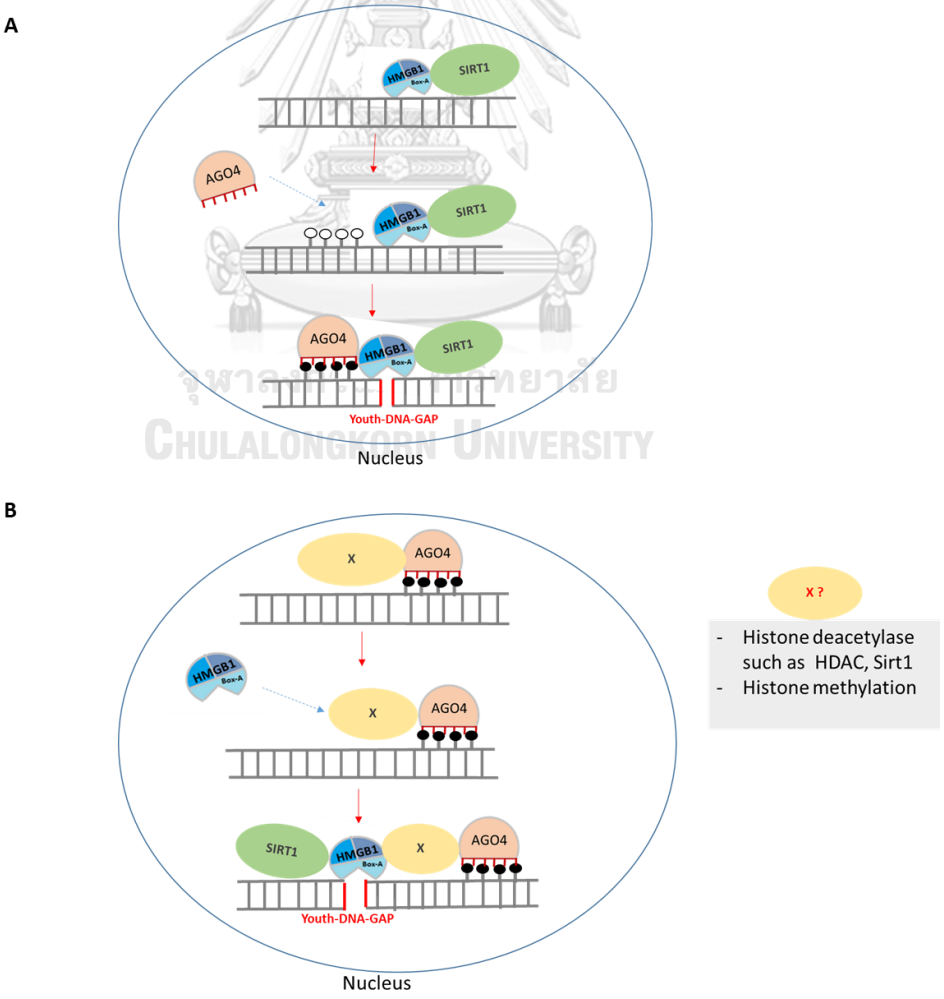

จุฬาลงกรณ์มหาวิทยาลัย
CHULALONGKORN UNIVERSITY

Figure 28. Schematic representation two hypotheses of how HMGB1 mediates DNA methylation preventing genomic instability. (A) HMGB1 interact with SIRT1, and then AGO4 de novo methylate DNA to generate an appropriate environment and allow Youth-DNA-GAP production by Box-A of HMGB1. (B) AGO4 and protein X form heterochromatin, and then recruit HMGB1 protein to produce Youth-DNA-GAP by Box-A domain which is interact with SIRT1 histone deacetylase.

จุฬาลงกรณ์มหาวิทยาลัย
Chulalongkorn University

จุฬาลงกรณ์มหาวิทยาลัย
Chulalongkorn University

REFERENCES

จุฬาลงกรณ์มหาวิทยาลัย
Chulalongkorn University

1. Vijg J, Suh Y. Genome instability and aging. Annual review of physiology. 2013; 75:645–668.

2. Hanahan D, Weinberg RA. Hallmarks of cancer: the next generation. Cell. 2011; 144:646-674.

3. Chen RZ, Pettersson U, Beard C, Jackson-Grusby L, Jaenisch R. DNA hypohylation leads to elevated mutation rates. Nature. 1998; 395(6697):89-93.

4. Beisel C, Paro R. Silencing chromatin: comparing modes and mechanisms. *Nat. Rev. Genet.* 2011; 12:123–135.

5. Ehrlich M. DNA hypomethylation in cancer cells. *Epigenomics*. 2009; **1**:239–259.

6. Ehrlich M. DNA methylation in cancer: too much, but also too little. *Oncogene*. 2002; 21:5400–5413.

7. Robertson KD. DNA methylation, methyltransferases, and cancer. Oncogene. 2001; 20:3139–3155.

8. Mills RE, Bennett EA, Iskow RC, Devine SE. Which transposable elements are active in the human genome?. Trends in genetics. 2007;23(4):183-191.

9. Pheasant M, Mattick JS. Raising the estimate of functional human sequences, Genome research. 2007;17(9):1245-1253.

10. Zhang X, Yazaki J, Sundaresan A, Cokus S, Chan SW, Chen H, et al. Genome-wide high-resolution mapping and functional analysis of DNA methylation in Arabidopsis. Cell. 2006;126:1189–1201.

11. Suzuki MM, Bird A. DNA methylation landscapes: provocative insights from epigenomics. Nature Review Genetic. 2008;9:465–476.

12. Mathieu O, Bender J. RNA-directed DNA methylation. Journal of cell science. 2004;117(21):4881-8.

13. Mahfouz MM. RNA-directed DNA methylation: mechanisms and functions. Plant signaling & behavior. 2010;5(7):806-16.

14 Hutvagner G, Simard MJ. Argonaute proteins: key players in RNA silencing. Nature reviews Molecular cell biology. 2008;9(1):22-32.

Chulalongkorn University

15 Erdmann RM, Picard CL. RNA-directed DNA Methylation. PLoS Genetic. 2020; 16(10): e1009034.

16. Chalertpet K, Pin-On P, Aporntewan C, Patchsung M, Ingrungruanglert P, Israsena N, et al. Argonaute 4 as an Effector Protein in RNA-Directed DNA Methylation in Human Cells. Front Genet. 2019; 10: 645.

17. Patchsung M, Settayanon S, Pongpanich M, Mutirangura D, Jintarith P, Mutirangura A. Alu siRNA to increase Alu element methylation and prevent DNA damage. Epigenomics. 2018;10 (2):175–185.

18. Pornthanakasem W, Kongruttanachok N, Phuangphairoj C, Suyarnsestakorn C, Sanghangthum T, Oonsiri S, Ponyeam W, et al. LINE-1 methylation status of endogenous DNA double-strand breaks. Nucleic acids research. 2008;36(11):3667-3675.

19. Thongsroy J, Matangkasombut O, Thongnak A, Rattanatanyong P, Jirawatnotai S, Mutirangura A. Replication-independent endogenous DNA double-strand breaks in Saccharomyces cerevisiae model. PloS one. 2013;8(8), e72706.

20. Kongruttanachok N, Phuangphairoj C, Thongnak A, Ponyeam W, Rattanatanyong P Pornthanakasem W, et al. Replication independent DNA double-strand break retention may prevent genomic instability. Molecular cancer. 2010;9(1):70.

21. Pongpanich M, Patchsung M, Thongsroy J, Mutirangura A. Characteristics of replication-independent endogenous double-strand breaks in Saccharomyces cerevisiae. BMC genomics. 2014;15(1):50.

22. Mutirangura A. A Hypothesis to Explain How the DNA of Elderly People Is Prone to Damage: Genome-Wide Hypomethylation Drives Genomic Instability in the Elderly by Reducing Youth-Associated Gnome-Stabilizing DNA Gaps. Intech open. 2018

23. Kang R, Zhang Q, Zeh HJ 3rd, Lotze MT, Tang D. HMGB1 in cancer: good, bad, or both? Clin Cancer Res. 2013;19:4046–4057.

24. He SJ, Cheng J, Feng X, Yu Y, Tian L, Huang Q. The dual role and therapeutic potential of highmobility group box 1 in cancer. Oncotarget. 2017;8:64534–64550.

25. Gent DC van, Hiom K, Paull TT, Gellert M. Stimulation of V(D)J cleavage by high mobility group proteins. EMBO Journal. 1997; 16(10): 2665–2670.

จุฬาลงกรณ์มหาวิทยาลัย
Chulalongkorn University

26. Dai Y, Wong B, Yen YM, Oettinger MA, Kwon J, Johnson RC. Determinants of HMGB Proteins Required To Promote RAG1/2-Recombination Signal Sequence Complex Assembly and Catalysis during V(D)J Recombination. Molecular cell Biology. 2005; 25(11): 4413–4425.

27. Prasad R, Liu Y, Deterding LJ, Poltoratsky VP. HMGB1 is a cofactor in mammalian base excision repair. Molecular cell. 2007;27: 829-841,

28. Giavara S, Kosmidou E, Hande MP, Bianchi ME, Morgan A, d'Adda di Fagagna F, et al. Yeast Nhp6A/B and mammalian Hmgb1 facilitate the maintenance of genome stability. Current biology. 2005;15(1):68-72.

29. Grabowska W, Sikora E, Bielak-Zmijewska A. Sirtuins, a promising target in slowing down the ageing process. Biogerontology. 2017;18(4):447–476.

30. Longo VD, Kennedy BK. Sirtuins in Aging and Age-Related Disease. Cell. 2006; 126(2): 257-268

31. Goodwin GH, Sanders C, Johns EW. A new group of chromatin-associated proteins with a high content of acidic and basic amino acids. Eur J Biochem. 1973;38(1):14-9.

32. He SJ, Cheng J, Feng X. The dual role and therapeutic potential of high-mobility group box 1 in cancer. Oncotarget. 2017; 8(38): 64534–64550.

33. Read CM, Cary PD, Crane-Robinson C, Driscoll PC, Norman DG. Solution structure of a DNA-binding domain from HMG1. Nucleic Acids Res. 1993; 21(15):3427-36.

34. Bustin M. Review Regulation of DNA-dependent activities by the functional motifs of the high-mobility-group chromosomal proteins. Mol Cell Biol. 1999; 19(8):5237-46.

35. Stros M. HMGB proteins: interactions with DNA and chromatin. Biochim Biophys Acta. 2010;1799(1–2):101–113.

36. Bianchi ME, Beltrame M, Paonessa G. Specific recognition of cruciform DNA by nuclear protein HMG1. Science. 1989;243(4894):1056–1059.

37. Diener KR, Al-Dasooqi N, Lousberg EL, Hayball JD. Review The multifunctional alarmin HMGB1 with roles in the pathophysiology of sepsis and cancer. Immunol Cell Biol. 2013 ; 91(7):443-50.

38. Yang H, Ochani M, Li J, Qiang X, Tanovic M, Harris HE, et al. Reversing established sepsis with antagonists of endogenous high-mobility group box 1. Proc Natl Acad Sci U S A. 2004; 101(1):296-301

39. Wang Q, Zeng M, Wang W, Tang J. The HMGB1 acidic tail regulates HMGB1 DNA binding specificity by a unique mechanism. Biochem Biophys Res Commun. 2007; 360(1):14-9.

40. Guo ZS, Liu Z, Bartlett DL, Tang D, Lotze MT. Life after death: targeting high mobility group box 1 in emergent cancer therapies. Am J Cancer Res. 2013; 3(1):1-20.

41. Wang S and Zhang Y. HMGB1 in inflammation and cancer. J Hematol Oncol. 2020

42. Hock R, Furusawa T, Ueda T, Bustin M. Review HMG chromosomal proteins in development and disease. Trends Cell Biol. 2007; 17(2):72-9.

43. Polanska E, Dobsakova Z, Dvorackova M, Fajkus J, Stros M. HMGB1 gene knockout in mouse embryonic fibroblasts results in reduced telomerase activity and telomere dysfunction. Chromosoma. 2012;121:419–31.

44. Giavara S, Kosmidou E, Hande MP, Bianchi ME, Morgan A, d'Adda di Fagagna F, et al. Yeast Nhp6A/B and mammalian Hmgb1 facilitate the maintenance of genome stability. Current biology. 2005;15(1):68-72.

45. Tubbs A, Nussenzweig A. Endogenous DNA Damage as a Source of Genomic Instability in Cancer. 2017;168: 644-656.

46. Mehta A, Haber JE. Sources of DNA double-strand breaks and models of recombinational DNA repair. Cold Spring Harb Perspect Biol. 2014; 6(9):a016428.

47. Roca J. Topoisomerase II: a fitted mechanism for the chromatin landscape. Nucleic Acids Res. 2009; 37(3):721–730.

48. Thongsroy J, Patchsung M, Pongpanic M, Settayanon S, Mutirangura A. Reduction in replication-independent endogenous DNA double-strand breaks promotes genomic instability during chronological aging in yeast. FASEB. 2018.

49. Zemach A, McDaniel IE, Silva P, Zilberman D. Genome-wide evolutionary analysis of eukaryotic DNA methylation. Science. 2010 328:916–919.

จุฬาลงกรณ์มหาวิทยาลัย
Chulalongkorn University

50. Li E, Zhang Y. DNA methylation in mammals. Cold Spring Harb Perspect Biol. 2014;6:a019133.

51. Bird AP. CpG-rich islands and the function of DNA methylation. Nature. 1986;321:209-13

52. Bollati V, Schwartz J, Wright R, Litonjua A, Tarantini L, Suh H, et al. Decline in genomic DNA methylation through aging in a cohort of elderly subjects. Mech. Ageing Dev. 2009;130:234–239

53. Deininger P. Alu elements: know the SINEs. Genome Biology volume. Genome Biol 2011; 12: 236

54. Dewannieux M, Esnault C, Heidmann T: LINE-mediated retrotransposition of marked Alu sequences. Nature Genetic. 2003; 35:41-48.

55. Eden,A., Gaudet,F., Waghmare,A. and Jaenisch,R. Chromosomal instability and tumors promoted by DNA hypomethylation. Science. 2003; 300:455

56. Kitkumthorn N, Tuangsintanakul T, Rattanatanyong P, Tiwawech D, Mutirangura A. LINE-1 methylation in the peripheral blood mononuclear cells of cancer patients. Clin Chim Acta. 2012;413:869-74.

57. Pobsook T, Subbalekha K, Sannikorn P, Mutirangura A. Improved measurement of LINE-1 sequence methylation for cancer detection. Clin Chim Acta. 2011;412:314-21

58. Jintaridth P, Mutirangura A. Distinctive patterns of age-dependent hypomethylation in interspersed repetitive sequences, Physiological genomics. 2010;41(2):194-200.

59. Jintaridth P, Tungtrongchitr R, Preutthipan S, Mutirangura A. Hypomethylation of Alu elements in post-menopausal women with osteoporosis. PLoS One. 2013;8(8):e70386.

60. Feinberg AP and Vogelstein B. Hypomethylation distinguishes genes of some human cancers from their normal counterparts. Nature. 1983;301:89–92.

61. Treangen TJ, Salzberg SL. "Repetitive DNA and next-generation sequencing: computational challenges and solutions". Nature Reviews Genetics. 2012;13(1):36–46.

62. Aguilera A, Gómez-González B. Genome instability: a mechanistic view of its causes and consequences. Nat Rev Genet. 2008;9:204–217.

63. Yao Y and Dai W. Genomic Instability and Cancer. J Carcinog Mutagen. 2014; 5: 1000165.

64. Ui A, Chiba N, Yasui A. Relationship among DNA double-strand break (DSB), DSB repair, and transcription prevents genome instability and cancer. Cancer Sci. 2020 ;111(5):1443-1451.

65. Wassenegger M, Heimes S, Riedel L, Sänger HL. RNA-directed de novo methylation of genomic sequences in plants, Cell. 1994;76(3):567-576.

66. Mathieu O, Bender J. RNA-directed DNA methylation. Journal of cell science. 2004;117(21):4881-8.

67. Hutvagner G, Simard MJ. Argonaute proteins: key players in RNA silencing. Nature reviews Molecular cell biology. 2008;9(1):22-32.

68. Zilberman D, Cao X, Jacobsen SE. ARGONAUTE4 control of locus-specific siRNA accumulation and DNA and histone methylation. Science. 2003;299 (5607):716–719.

69. Erdmann RM, Picard CL. RNA-directed DNA Methylation. PLoS Genetic. 2020;16(10): e1009034.

70. Cuerda-Gil D, Slotkin RK. Non-canonical RNA-directed DNA methylation. Nature plants. 2016;2(11):16163.

71. Yang N, Kazazian HH Jr. L1 retrotransposition is suppressed by endogenously encoded small interfering RNAs in human cultured cells. Nat Struct Mol Biol. 2006; 13(9):763-71.

72. Castanotto D, Tommasi S, Li M, Li H, Yanow S, Pfeifer GP, et al. Short hairpin RNA-directed cytosine (CpG) methylation of the RASSF1A gene promoter in HeLa cells. Mol. Ther. 2005;12(1):179–183.

73. Lindahl T, Barnes DE. Repair of endogenous DNA damage. Cold Spring Harb. Symp. Quant. Biol. 2000:127-133.

74. Tubbs A, Nussenzweig A. Endogenous DNA Damage as a Source of Genomic Instability in Cancer. 2017; 168(4):644-656.

75. Ramstein J and Lavery R. Energetic coupling between DNA bending and base pair opening. Proc Natl Acad Sci U S A. 1988; 85(19):7231-7235.

จุฬาลงกรณ์มหาวิทยาลัย
CHULALONGKORN UNIVERSITY

76. Teves SS and Henikoff S. DNA torsion as a feedback mediator of transcription and chromatin dynamics. Nucleus. 2014;5(3):211-218.

77. Oberstrass FC, Fernandes LE, Lebel P, and Bryant Z. Torque spectroscopy of DNA: base-pair stability, boundary effects, backbending, and breathing dynamics. Phys Rev Lett. 2013;110(17):178103.

78. McCauley MJ, Zimmerman J, Maher LJ 3rd, Williams MC. HMGB binding to DNA: single and double box motifs. J Mol Biol. 2007;374(4):993-1004.

79. Davalos AR, Kawahara M, Malhotra GK, Schaum N, Huang J, Ved U, et al. p53-dependent release of Alarmin HMGB1 is a central mediator of senescent phenotypes. J Cell Biol. 2013; 201(4): 613-629.

80. Vanessa V, Simona G, Michael F, Monica N, Stefano B. γH2AX as a marker of DNA double strand breaks and genomic instability in human population studies. Mutation research. 2013;753(1):24-40.

จุฬาลงกรณ์มหาวิทยาลัย
CHULALONGKORN UNIVERSITY

VITA

NAME	Papitchaya Watcharanurak
DATE OF BIRTH	18 August 1989
PLACE OF BIRTH	Bangkok
INSTITUTIONS ATTENDED	Faculty of Medical technology, Prince of Songkhla University Department of Biomedical sciences, Faculty of Medicine, Prince of Songkhla University
HOME ADDRESS	94/94 Kanchanavanich road MuangSongkhla Songkhla 90000
PUBLICATION	-
AWARD RECEIVED	-

จุฬาลงกรณ์มหาวิทยาลัย
CHULALONGKORN UNIVERSITY

จุฬาลงกรณ์มหาวิทยาลัย
Chulalongkorn University